

Eccentricity Evolution of Extrasolar Multiple Planetary Systems due to the Depletion of Nascent Protostellar Disks

M. Nagasawa^{1,2}, D. N. C. Lin¹, and S. Ida³

mnagasawa@mail.arc.nasa.gov, lin@ucolick.org, ida@geo.titech.ac.jp

ABSTRACT

Most extrasolar planets are observed to have eccentricities much larger than those in the solar system. Some of these planets have sibling planets, with comparable masses, orbiting around the same host stars. In these multiple planetary systems, eccentricity is modulated by the planets' mutual secular interaction as a consequence of angular momentum exchange between them. For mature planets, the eigenfrequencies of this modulation are determined by their mass and semi-major axis ratios. But, prior to the disk depletion, self gravity of the planets' nascent disks dominates the precession eigenfrequencies. We examine here the initial evolution of young planets' eccentricity due to the apsidal libration or circulation induced by both the secular interaction between them and the self gravity of their nascent disks. We show that as the latter effect declines adiabatically with disk depletion, the modulation amplitude of the planets' relative phase of periape is approximately invariant despite the time-asymmetrical exchange of angular momentum between planets. However, as the young planets' orbits pass through a state of secular resonance, their mean eccentricities undergo systematic quantitative changes. For applications, we analyze the eccentricity evolution of planets around Upsilon Andromedae and HD168443 during the epoch of protostellar disk depletion. We find that the disk depletion can change the planets' eccentricity ratio. However, the relatively large amplitude of the planets' eccentricity cannot be excited if all the planets had small initial eccentricities.

¹UCO/Lick Observatory, University of California, Santa Cruz, CA 95064, U.S.A.

²Present address: Space Science Division, MS 245-3, NASA Ames Research Center, Moffett Field, CA 94035-1000, U.S.A.

³Department of Earth and Planetary Sciences, Tokyo Institute of Technology, Meguro-ku, Tokyo 152-8551, Japan

Subject headings: planetary systems: formation — celestial mechanics — stars: individual (Upsilon Andromeda, HD168443) — planetary systems: protoplanetary disks — extra solar planets

1. INTRODUCTION

Many extrasolar planetary systems have been discovered recently using the radial velocity technique (Marcy & Butler 2000). The basic assumption is that the spectroscopic variations observed in some targeted stars are due to the Doppler shift associated with the reflex motion of stars with unseen companions. The mass of these companions depends on the poorly known inclination of these systems. But, unless the orbits of these systems are highly inclined (Stepinski & Black 2001), the inferred masses of the companions are comparable to that of Jupiter. The observed spectra of some targeted stars indicate the presence of multiple companions around them. For example, three companions are found to orbit around Upsilon Andromedae. The long term stability of this system requires their inclination to be sufficiently small such that the masses of these companions are no more than a few Jupiter mass (M_J) and much smaller than that of their host star (Laughlin & Adams 1999; Rivera & Lissauer 2000; Stepinski, Malhotra, & Black 2000; Ito & Miyama 2001; Lissauer & Rivera 2001). Two companions are also found around HD168443 with minimum masses which are an order of magnitude larger than M_J . Although the masses of these companions would be a modest fraction of a solar mass (M_\odot) if this system is viewed nearly face on, such compact hierarchical stellar systems have not been seen before. Thus, we follow the conventional practice to refer these multiple companions as planets.

In the limit that the planets' masses are substantially smaller than that of their host star, their mutual secular perturbation induces them to exchange angular momentum while preserving their energy. (Planets in mean motion resonances also exchange energy on comparable time scales). Around Upsilon And and HD168443, the planets' orbits are not in mean motion resonances so that their semi-major axes are conserved while their eccentricity and longitude of periastron modulate over some characteristic secular time scale (Murray & Dermott 1999).

But, the secular perturbation between the planets has not always been sustained at the present level. During the epoch of their formation, protoplanets are embedded in protostellar disks which have been found around most young stellar objects (cf. Haisch, Lada, & Lada 2001). The mass and temperature distribution of these disks are very similar to those inferred from the minimum mass nebula model for the solar system (Beckwith 1999). The self gravity of these disks can induce the orbits of planets formed within them to precess at a rate faster

than that due their mutual perturbation. Consequently, the rate of angular momentum transfer between the interacting planets is suppressed.

In the solar system, the initial contribution of the solar nebula to the total gravitational potential dominates the precession frequency of asteroids and comets over that due to the secular perturbation induced on them by the giant planets. The planets also undergo precession induced by the disk gravity and other planets' secular perturbation. In general the precession frequencies of these celestial bodies do not equal each other. But as gas is depleted in the solar nebula, its self gravity weakens. The total precession frequencies of both the asteroids and the planets declines, though at a different rate. When the precession frequency of asteroids with some semi major axes coincides with that of a major planet, they enter into a state of secular resonance. In this resonance, the eccentricity of the asteroids is either excited or damped monotonically, depending on their relative longitude of periastron passage with respect to that of the planet. As this secular resonance sweeps across the solar system, large eccentricity may be excited among some small celestial bodies (Ward, Colombo, & Franklin 1976; Heppenheimer 1980; Nagasawa, Tanaka, & Ida 2000; Nagasawa & Ida 2000).

In this paper, we examine the effects of disk depletion on the eccentricity evolution of the planetary systems around Ups And and HD168443. Through such an investigation, we hope to infer the kinematic properties which these planets are born with and thereby cast constraints on their formation process. In §2, we briefly discuss the precession due to the secular interaction between planets and that due to the self gravity of the protostellar disk. The conditions for secular resonance are discussed. We introduce, in §3, a working model and describe the method we used to analyze the eccentricity evolution. In §4, we present the results of some calculations. We use these numerical results to demonstrate the evolution of these systems with Hamiltonian contour maps. Based on these results, we infer, in §5, some implications on the planets' orbital eccentricity shortly after their formation and while they are still embedded in their nascent disks. Finally, we summarize our results in §6.

2. SECULAR INTERACTION IN MULTIPLE EXTRASOLAR PLANETARY SYSTEMS

2.1. Current Orbital Properties

In this paper, we focus our discussion on the planets around Upsilon Andromeda (c and d) and those around HD168443. The decomposition of Upsilon Andromeda's spectra indicate that there are three planets orbiting around it (Butler et al. 1999). Inferred orbital

elements⁴ of the Upsilon Andromeda planets are shown in Table 1(a). The semi-major axis, the eccentricity, the longitude of periastron, mass of the planet, and periastron passage time (JD) are denoted by a , e , ϖ , M , and T_{peri} , respectively. The subscripts b , c , and d represent the values for the individual planets. Throughout this analysis, we assume that these systems are viewed edge-on and their masses correspond to their minimum values. Provided their orbits are coplanar, our analysis is independent of the planets’ inclination. Our approach becomes inadequate for the limiting cases of nearly face-on orbits where the masses of the companions are comparable to their host stars.

Around Ups And, the eccentricity of the innermost planet b is essentially undetectable. The orbit of planet b is likely to be circularized during the main sequence life span of the host star Ups And by the tidal dissipation within the planet’s interior as expected for Jupiter-like extrasolar planets with semi-major axis less than 0.05 AU (Rasio et al. 1996). With its low mass and small semi-major axis, planet b does not contribute significantly to the dynamical evolution of the system (Mardling & Lin 2003). Although the outer planets (c and d) still exert secular perturbation on planet b , the cumulative effect on its eccentricity modulation is limited. Under the present configuration, the secular interaction of planet b with planets c and d is weakened by the rapid precession due to the post-Newtonian relativistic correction in the gravitational potential of the host star (Mardling & Lin 2003). Neglecting the secular perturbation due to planet b , the orbital evolution of planets c and d obtained from the direct orbital integration of the full equation of motion is shown in Figure 1a. In the numerical integration, the calculation is started with the eccentricity ratio $x \equiv e_c/e_d$ and the relative longitude of periastrons between planets c and d , $\eta \equiv \varpi_c - \varpi_d$, based on their observed values 0.66 and ~ -0.06 radian, respectively. We compute the evolution of the system for over 2×10^4 years. The equi-Hamiltonian contours (see Appendix D) are also shown. For planets c and d around Ups And, the massive planet d has larger eccentricity than smaller planet c . The longitudes of periastron of planet c and d are always close to each other. When the planets are in librating (closed) track in $(x-\eta)$ diagram, the planetary system tends to be stable for a long time. The stabilities of this system around Ups And are well investigated (Laughlin & Adams 1999; Rivera & Lissauer 2000; Stepinski et al. 2000; Barnes & Quinn 2001; Ito & Miyama 2001; Lissauer & Rivera 2001; Chiang, Tabachnik, & Tremaine 2002; Mardling & Lin 2003).

Around HD168443, two massive planets are inferred from the radial velocity curves (Marcy et al. 2001). The best-fit orbital elements are shown in Table 1(b). We also numerically integrate the present-day orbital evolution of the planets b and c around HD168443. In

⁴<http://exoplanets.org/almamacframe.html>

contrast to the planetary system around Ups And, the lower mass planet b around HD168443 system, has an eccentricity which is more than twice that of the massive planet c. The orbits are integrated over 2.5×10^4 years, starting with $x = 2.65$ and $\eta \sim 1.92$ radian. These planets evolve in circulating (open) track in the $(x-\eta)$ diagram (Fig. 1b) and η evolves from $-\pi$ to π over a period of about 1.6×10^4 years. This system too is stable despite the large magnitude of eccentricity of planet b. The origin of such large mass and eccentricity of planets in this system has not been addressed previously.

2.2. Secular Perturbation between Two Planets

The secular interaction induces eccentricity modulation between planets c and d around Ups And (Laughlin & Adams 1999; Rivera & Lissauer 2000; Ito & Miyama 2001; Mardling & Lin 2003). For presentation purpose, it is useful to briefly recapitulate the analysis of secular interaction between two planets. It is customary to consider the secular (long-term) evolution of the interacting planets' orbits using a disturbing function (Murray & Dermott 1999). To the *lowest order*, the modulation of the eccentricity ($e_{c,d}$) and longitude of periapse ($\varpi_{c,d}$) of some planets c and d can be approximated by

$$\frac{de_{c,d}}{d\tau} = \gamma_{c,d} C e_{d,c} \sin(\varpi_{c,d} - \varpi_{d,c}) + \Lambda_{c,d}^e, \quad (1)$$

$$\frac{d\varpi_{c,d}}{d\tau} = \gamma_{c,d} \left(1 + C \left(\frac{e_{d,c}}{e_{c,d}} \right) \cos(\varpi_{c,d} - \varpi_{d,c}) \right) + \Lambda_{c,d}^\varpi + N_{c,d}, \quad (2)$$

where $\tau \equiv t/t_c$, t is the real time, $t_c = (4/n_c)(M_*/M_d)(a_d/a_c)^2/b_{3/2}^{(1)}$, $b_s^{(j)}(\alpha)$ are the Laplace coefficients with $\alpha = a_c/a_d$, M_c , M_d , and M_* are the mass of planets c, d, and the host star respectively, a_c and a_d are the semi-major axes of planets c and d respectively, $n_{c,d} = (GM_*/a_{c,d}^3)^{1/2}$ is the mean motion of planet c or d, $\gamma_{c,d} \equiv (a_c/a_{c,d})^{1/2}(M_c/M_{c,d})$ so that $\gamma_c = 1$, $C \equiv -b_{3/2}^{(2)}/b_{3/2}^{(1)}$ (Mardling & Lin 2002), $\Lambda_{c,d}^e$ is the change rate of eccentricity due to the non axisymmetric torque, $\Lambda_{c,d}^\varpi$ is the change rate of ϖ due to the non axisymmetric torque, and $N_{c,d}$ is axisymmetric modification of the gravitational potential. When $a_c/a_d \ll 1$, $t_c = (4/3n_c)(M_*/M_d)(a_d/a_c)^3$ and $C = -5a_c/4a_d$. Frequently used variables are tabulated in Table 2. The planets' secular interaction induces both axisymmetric and non axisymmetric perturbations on each other. While only the non axisymmetric component of the planets' secular perturbation on each other can lead to angular momentum exchange and $e_{c,d}$ modulations in equation (1), both axisymmetric and non axisymmetric perturbations contribute to the evolution of $\varpi_{c,d}$ through the first and second term on the right hand side of equation (2) respectively. These linearized equations of secular motion, though only accurate to the first order, are useful for obtaining analytic-approximation solutions which

highlight the dominant physical effects. For the numerical calculation of the planets’ orbits (see §4), we use the exact equation of planets’ motion.

Planet-disk interaction also leads to both axisymmetric modification of the gravitational potential ($N_{c,d}$) and non axisymmetric torque ($\Lambda_{c,d}^{e,\varpi}$) (Goldreich & Tremaine 1980, 1982; Lin & Papaloizou 1986 a, b, 1993). For the latter effect, planets excite waves in the disk which carry angular momentum. The dissipation of these waves, anywhere in the disk, would result in a finite torque (Papaloizou & Lin 1984). In principle, the net torque vanishes in the inviscid limit. However, their amplitude grows and steepens into nonlinear shocks as the waves propagate away from the location where they are launched, leading to an effective torque (Savonije, Papaloizou, & Lin 1994). The evolution of the axisymmetric potential modifies the precession of ϖ but do not directly influence the eccentricity of the orbits (see eq. [2]). While the non axisymmetric torque may induce monotonic changes in e (Chiang & Murray 2002) and ϖ (see eq. [1]), the magnitude and sign of $\Lambda_{c,d}^e$ depends sensitively on the disk structure. Interaction between the embedded planets with disk gas through corotation resonances damps the eccentricity while that through Lindblad resonances excites the eccentricity (Goldreich & Tremaine 1980). For protoplanets with mass less than a few times that of Jupiter and modest eccentricity, gas may flow in the vicinity of their orbits such that the eccentricity damping effect of the corotation resonances is stronger than the excitation effect of the Lindblad resonances (Goldreich & Tremaine 1980). But protoplanets with masses an order of magnitude larger than that of Jupiter may open relatively wide gaps in protostellar disks. In this limit, the protoplanets’ corotation resonances may be cleared of disk gas such that their eccentricity may be excited (Artymowicz 1993; Papaloizou, Nelson, & Masset 2001; Goldreich & Sari 2002). For precession, the contribution from the non axisymmetric torque may be weaker than that due to the disk’s axisymmetric contribution to the total gravitational potential in the limit that the torque resulting from the planets’ interaction with the interior and exterior regions of the disk are balanced or in low-viscosity and thin disks where planets with relatively low masses can open wide gaps. However, the non axisymmetric torque may lead to significant contributions over time in relatively massive disks.

In order to analyze the contribution of each effect, we adopt a piece meal approach. In this paper, we focus our attention on the evolution of planetary orbits due to the changes in the axisymmetric disk potential. For the departure from a point-mass potential, the apsidal motion of planets c and d are included in $N_{c,d}$ (see Appendix A). In this first step, we neglect the effects due to the non axisymmetric torque by setting $\Lambda_{c,d}^{e,\varpi} = 0$ in equations (1) and (2). The extension of our discussion to the limit of finite non axisymmetric torque will be presented in a future contribution.

2.3. Precession Frequencies

To the lowest order, the solution of equations (1) and (2) can be expressed as

$$e_{c,d} \exp(i\varpi_{c,d}) = A_{c,d} \exp\{i(g_1 t + \beta_1)\} + B_{c,d} \exp\{i(g_2 t + \beta_2)\}, \quad (3)$$

where $A_{c,d}$ and $B_{c,d}$ are the oscillation amplitudes, β_1 and β_2 are the phase angles (e.g., Brouwer & Clemence 1961). The individual planet's longitudes of periastrons precess with two independent eigenfrequencies,

$$g_{1,2} = \frac{1}{2} \left\{ g_c + g_d \pm [(g_c - g_d)^2 + 4g_{cd}^2]^{1/2} \right\}, \quad (4)$$

where

$$g_{c,d} \equiv \frac{\gamma_{c,d} + N_{c,d}}{t_c}, \quad g_{cd} \equiv \frac{C\gamma_d^{1/2}}{t_c} \propto (M_c M_d)^{1/2}. \quad (5)$$

From equation (2), we find that g_c would be the precession frequency of planet c if it is massless and is subjected to the secular perturbation of a massive planet d with a circular orbit. Similarly, g_d would be the precession frequency of planet d if it is massless and is subjected to the secular perturbation of a massive planet c with a circular orbit.

In the limit that $A_{c,d}$ and $B_{c,d}$ have comparable magnitudes and the two eigenfrequencies, $g_{1,2}$ have sufficiently large differences, the relative longitude of the two planets would circulate. Precessional degeneracy occurs when $g_1 = g_2$ so that the two planets precess synchronously regardless of the amplitude of their e and ϖ . In this degenerate state, the relative phase of the two planets' longitude of periape passage, $\eta \equiv \varpi_c - \varpi_d$, retains a constant value and the two planets are in a state of secular resonance. In this secular resonance, angular momentum is monotonically transferred from one planet to another because the relative orientation of their periastrons is maintained indefinitely. To lowest order, the planets' individual energy is conserved. With the exception of the special configuration in which $\eta = 0$ or $\pm\pi$, this monotonic transfer generally leads to eccentricity excitation of the angular momentum losing bodies and eccentricity damping of the angular momentum gaining bodies. In celestial mechanics, secular resonance is thought to be important in the current eccentricity distribution of the asteroids (Williams 1969).

From equation (4), we find that the magnitude of the difference between g_1 and g_2 is

$$\Delta g_{12} \equiv |g_1 - g_2| = [(g_c - g_d)^2 + 4g_{cd}^2]^{1/2} = \left[\left(\frac{1 - \gamma_d + \Delta N}{\tau_c} \right)^2 + 4g_{cd} \right]^{1/2}, \quad (6)$$

which vanishes on the exact center of secular resonance (where $g_1 = g_2$) only if $g_c = g_d$ and $g_{cd} = 0$. The former requirement corresponds to a necessary resonance condition $A_1 = 0$

where

$$A_1 \equiv 1 - \gamma_d + \Delta N \quad (7)$$

is the precession rate induced by axisymmetric component of the perturbed potential (see eq. [9] below). The latter requirement is satisfied if either $M_c = 0$ or $M_d = 0$ (see eq. [5]). Equation (6) implies that planets with comparable masses cannot have precessional degeneracy with $g_1 = g_2$ (Kinoshita & Nakai 2000).

The present value of γ_d is 0.29 for planets c and d around Ups And. Today, in the absence of any residual disk ($N_{c,d} = 0$), $g_2 \sim g_d < g_1 \sim g_c$ and the outer two planets of Ups And are *not* in a state of precessional degeneracy. Nevertheless, their present orbits can be approximated by equation (3) with the magnitude of $A_{c,d}$ much smaller than that of $B_{c,d}$. Thus, the two planets primarily precess with eigenfrequency g_1 and their relative longitudes of periastrons librate over a restricted range of phases. This phase lock is equivalent of a state of secular resonance. This resonant interaction is the result of a dynamical feedback through the planets' secular interaction.

2.4. Three Classes of Relative Orbits

In order to illustrate the importance of this feedback effect, we substitute $x \equiv e_c/e_d$ and $\eta \equiv \varpi_c - \varpi_d$, equations (1) and (2) reduce to

$$\frac{dx}{d\tau} = C(1 + \gamma_d x^2)\sin\eta, \quad (8)$$

$$\frac{d\eta}{d\tau} = (1 - \gamma_d) + (C/x)(1 - \gamma_d x^2)\cos\eta + \Delta N = A_1 + A_2(x)\cos\eta, \quad (9)$$

where $\Delta N \equiv N_c - N_d$, A_1 is given in equation (7), and $A_2(x) \equiv (C/x)(1 - \gamma_d x^2)$ is introduced for notational simplicity. There are three families of relative orbits which can be illustrated below with the linearized approximation solutions of equations (8) and (9) (see Appendix B). We show below that the relative magnitude of A_1 and A_2 determine the nature of the orbits.

1) *Circulation*. In these solutions, the magnitude of x modulates about some values x_0 such that $x = x_0 + \delta x(\tau)$ with an amplitude $|\delta x(\tau)| \ll x_0$ for all values of η which ranges between 0 and 2π . In the limit that $|A_1| \gg |A_2|$, η decreases monotonically (because $A_1 < 0$) while δx oscillates (see solutions in eqs. [B7] and [B8] in Appendix B.2). To the lowest order these solutions reduce to

$$\eta \simeq A_1 \tau, \quad \delta x \simeq -\frac{C}{A_1} \cos A_1 \tau. \quad (10)$$

Near the secular resonance where $|A_1|$ is relatively small, the amplitude of δx becomes large.

2) *Libration.* In the opposite limit that $|A_1| \ll |A_2|$, the non axisymmetric secular interaction between the planets is important. There are stationary points in the $(x-\eta)$ plane which center on the values of $x = x_m$ and $\eta = 0$ or π (see Appendix B.1). Around these points, there are orbits with both small amplitude modulation such that

$$\epsilon \equiv \frac{x - x_m}{x_m} = \epsilon_0 \sin \omega \tau, \quad \eta = \eta_0 \cos \omega \tau, \quad (11)$$

where

$$\eta_0 = \pm \epsilon_0 \quad \text{and} \quad \omega = \pm \frac{C}{x_m} (1 + \gamma_d x_m^2) \quad (12)$$

is the oscillation frequency (see Appendix B.1). The dimensionless amplitude of these librational orbits $\epsilon_0 \ll 1$. For these orbits, although $g_1 \neq g_2$, secular interaction induces them to precess at similar frequencies that their relative longitude of periaapse passage is always approximately aligned or anti aligned. Thus, these planets are effectively in a state of secular resonance. Note that because the libration is centered around $\eta = 0$ or π , there is no effective angular momentum transfer despite the phase lock.

3) *Excitation.* For systems with $|A_1| < |A_2|$, there are also orbits in which x and η have very different values as x_m and 0 (or π) respectively. In these cases, η would evolve rapidly to a phase angle

$$\eta_1 \simeq \cos^{-1} \left(-\frac{A_1}{A_2} \right) = \cos^{-1} \left(\frac{-A_1 x}{C(1 - \gamma_d x^2)} \right), \quad (13)$$

such that $d\eta/d\tau$ is reduced to zero (see eq. [9]) and the two planets become phase locked.

For all non zero (or π) values of η_1 , the monotonic increases/decreases of x correspond to eccentricity excitation/damping, analogous to the situation of precessional degeneracy. In this state of near secular resonances, angular momentum is monotonically transferred from one planet to the other, resulting in a monotonic evolution of x . The modification of x in turn leads to an evolution in η . Along the path of x and η_1 evolution, $g_1 \neq g_2$ and the planets would librate about their evolving guiding center. For the special cases when the two planets enter the resonance, the second order solution reduces to that in equation (11) and all orbits become instantaneously librational, even though ϵ_0 and η_0 may become arbitrarily large. At the center of resonance where A_1 , A_2 , and A_1/A_2 all vanish, $\eta_1 = \pi/2$ and x_m evolves exponentially. We discuss the evolution of these systems in Appendix C.

3. MODELS

The above analytic approximation is useful for isolating the three family of orbits along with two stationary points in the $(x-\eta)$ diagram. These orbits generally follows the contours of equi Hamiltonian map (see Appendix D). However, the topological evolution of the Hamiltonian map alone is insufficient for the determination of the planets' orbits during the depletion of the disk. We carry out, below, numerical integration of the *full* equation of motion for the planets subject to the potential of their host star and nascent disks. In this section, we briefly describe a model prescription with which we examine the passage of librational degeneracy during the epoch of disk depletion.

3.1. Planetary Formation Scenarios and Disk Model

We first discuss the physical process of disk depletion. According to conventional theories, planets are formed through the condensation of grains which grow to planetesimals via cohesive collisions (Hayashi, Nakazawa, & Nakagawa 1985; Lissauer 1987; Wetherill 1990). Upon attaining a sufficiently large mass, planetesimals accrete gas (Mizuno 1980; Bodenheimer & Pollack 1986; Pollack et al. 1996). Eventually, their growth is terminated when protoplanets can tidally induce the formation of a gap near their orbit (Goldreich & Tremaine 1980; Lin & Papaloizou 1980, 1993; Takeuchi, Miyama, & Lin 1996).

Thereafter, gas in the inner of the disk continues to diffuse inward as it loses angular momentum to the planet. Since gas replenishment is cut off by the formation of the gap, the inner region is depleted well before the outer region of the disk. For the present discussions, we assume that the mass in the inner regions of the disk becomes negligible by the stage when the second planet is fully grown. Thus, in our analysis of planets' dynamical evolution, we only need to consider their interaction with the disk region extended outside the outer planet. Both the gravitational and tidal influences of the disk on the outer planet are much more intense than on the inner planet because the former is much closer to where most of the gas is distributed.

When the planets' orbits lie in the same plane as their nascent disks and their distance to the nearest edge of their nascent disks is greater than the disks' scale height, a thin-disk approximation is sufficient for the computation of the disks' gravitational potential. Following the approach of Ward (1981), the self-gravitating potential for a disk model with a surface density profile $\Sigma = \Sigma_0(r_0/r)^k$ (with Σ_0 and r_0 being some fiducial values) can be

expressed as

$$V(r) = 2\pi G \Sigma_0 r \left(\frac{r_0}{r}\right)^k \sum_{n=0}^{\infty} \left(\frac{A_n}{2n+k-1}\right) \left(\frac{r}{r_{\text{edge}}}\right)^{2n+k-1}. \quad (14)$$

In the above expression, r is the instantaneous location (rather than the semi major axis) of the planet. We also assume that the disk has an inner edge which is located at r_{edge} , interior to which $\Sigma = 0$. The coefficient $A_n = \{(2n)!/2^{2n}(n!)^2\}^2$. For illustration purpose, we consider the minimum mass solar nebula model (Hayashi 1981), in which $k = 3/2$. The general applicability of this phenomenological model for protostellar disks around different stars is questionable. In the absence of a reliable prescription, we parameterize disk models with a range of values in k (see §4.3). We assume the disk is extended to infinite and the semi-major axes of planets do not change as a consequence of disk depletion or planets' secular interaction with each other. The results to be presented below show that while the overall dynamical evolution of the planets' orbit is insensitive to the detailed disk model, the planets' extrapolated initial eccentricity ratio does depend on the mass of the disk gas near their orbits.

3.2. Planetary System and Prescription for Disk Depletion

For computational simplicity, we consider a planetary system consists of two planets with coplanar orbits. In the case of the Upsilon Andromeda system, we are concerned with gravitational interaction between planets c and d and neglect the contribution by planet b. We also neglect the influence of the planet's tidal interaction with the disk. Only the axisymmetric component of the disk potential is taken into account. Mutual inclinations between the two planets and between the planet and the disk are neglected. The inclination of the orbital plane is denoted by i . We take surface density of the disk as $5 \times \sin i$ times that of the minimum mass solar nebula model. Only the ratios, rather than the individual values, of the planets' and the disks' masses determine the planets' motion. Thus, our results do not depend on the inclination of the system (except for small changes in the mean motion and the long term dynamical stability for exceptional small values of i).

For models with different values of k , we scale Σ such that its value at the disks' inner edge r_{edge} remains invariant. As we have indicated above, inner region of the disk is likely to be severely depleted prior to the emergence of the second planet. Thus, we assume the disk depletion to proceed in an inside out manner by adopting a model in which the location of nebula inner edge (r_{edge}) is prescribed to expand outwards as $r_{\text{edge}}(t) = r_{\text{edge}}(t=0) + r_i t / t_{\Delta N}$ with $r_i = 1\text{AU}$ while Σ_0 is kept constant. In order to demonstrate that the passage of the secular resonance does not depend on the detailed prescription of the depletion process or

the structure of the disk, we also consider a model in which the surface density of the disk is assumed to decline by an identical reduction factor everywhere such that $\Sigma_0(t) = \Sigma_0(t = 0) \exp(-t/t_{\Delta N})$ with $r_{\text{edge}} = \text{constant}$. In the limit that $a_c/a_d \ll 1$ and $a_{c,d}/r_{\text{edge}} \ll 1$, we find that the two prescriptions of the disk depletion do not lead to a significant difference in the numerical results because $\Delta N \propto \Sigma/r_{\text{edge}}^{5/2}$. For the approximate prescription of ΔN (see eq. [D2]), the magnitude of $A_1 = 1 + \Delta N - \gamma_d$ changes on a time scale $\tau_{A_1} \sim t_{\Delta N}$ and the condition of the secular resonance $A_1 = 0$ is satisfied when

$$\frac{\Sigma_0 r_0^{3/2}}{r_{\text{edge}}^{5/2}} \simeq \frac{5(\gamma_d - 1) M_d}{4\pi a_d^3} \left(1 - \frac{n_c}{n_d}\right)^{-1}. \quad (15)$$

This condition can be attained with both prescriptions.

The orbital evolution of the planets can be directly integrated numerically, including the point-mass potential of the host stars and sibling planets as well as the contribution from the disk potential where the gravity can be expressed as

$$F = \frac{dV}{dr} = 2\pi G \Sigma(r, t) \sum_{n=0} \frac{4n}{4n+1} A_n \left(\frac{r}{r_{\text{edge}}(t)}\right)^{2n+1/2}, \quad (16)$$

where $k = 3/2$ is assumed.

4. RESULT OF NUMERICAL COMPUTATION

4.1. Evolution of Librating Planets Around Ups And

Using the equi-Hamiltonian contour maps, we illustrate the orbital evolution of planets c and d during disk depletion. Figure 2 shows the time evolution of the equi-Hamiltonian map of Upsilon Andromeda system. In these calculations, we adopt the mass ratio $M_c/M_d = 0.502$ based on the assumption that they occupy the same orbital plane. The nebula edge retreats from inside to outside (from panel 1 to panel 5). When the nebula edge is at 4.2AU (panel 1), the orbits librate around $(x = 10, \eta = 0)$ or $(x = 0.4, \eta = \pm\pi)$. The precession speed of the longitude of planet c’s periastron is slower than that of planet d’s periastron except for the occasional regressions. Embedded within such a disk, a pair of planets with the present observed values of x and η would not follow a closed librating track. When the nebula edge is at 5AU (panel 2), the two eigenfrequencies of the system become closer to each other. The eccentricities of planets modulate with large amplitudes. The magnitude of x librates on a closed equi-Hamiltonian track, about a central point at $x \sim 3.3$ and $\eta = 0$.

From the estimation of the equation (D2), we find that $A_1 = 1 + \Delta N - \gamma_d$ vanishes when the disk is retreated to $r_{\text{edge}} = 5.5\text{AU}$, namely, secular resonance occurs at $r_{\text{edge}} =$

5.5AU. The panel (3) represents the epoch of secular resonance passage. At this stage, the precession frequencies of the longitudes of periastrons nearly match with each other (*i.e.*, $\dot{\eta} \sim 0$ compared with \dot{x}). Consequently, η varies slowly (with finite values other than 0 or π) in comparison with the non negligible evolution of x such that the eccentricities can change significantly. The equi-Hamiltonian map is locally symmetric about the lines of $\eta = -\pi$, $-\pi/2$, 0, $\pi/2$, and π and that of $x = \gamma_d^{-1/2} \sim 2$.

When the nebula edge is beyond 5.5AU, the precession speed of longitude of planet c’s periastron is faster than that of planet d’s periastron (except for the occasional regressions). Panel (4) shows the case that the nebula edge has retreated to 7AU. The centers of the closed libration tracks are reversed from the situation in panels (1) and (2). The planetary configuration with $e_c > e_d$ and $\varpi_c \sim \varpi_d$ in panel (2) becomes that with $e_c < e_d$ and $\varpi_c \sim \varpi_d$ in panel (4). When the entire protoplanetary disk is depleted (panel (5)), stable orbits librate around ($x = 0.5$, $\eta = 0$) or ($x = 7$, $\eta = \pm\pi$). The shape of equi-Hamiltonian map is turned upside down with $x = \gamma_d^{-1/2}$. Figure 3 is the time evolution of the equi-Hamiltonian map for the uniform-depletion prescription with $r_{\text{edge}} = 4.5\text{AU}$. In this model, the secular resonance occurs when $\Sigma_0(t)/\Sigma_0(t = 0) = 0.5$. Although the time of the secular-resonance passage is slightly modified from that obtained with the model of inside-out depletion, the general evolutionary pattern is not qualitatively changed.

We also numerically integrate the orbits of planets c and d using the the same inside-out disk depletion prescription as above (*i.e.*, we arbitrarily set the initial disk edge to be at 4.2 AU and specify its retreating speed to be $10^{-5}\text{AU year}^{-1}$). We consider two sets of initial conditions. Figures 4a and c illustrate the evolution of a model with initial values of $x = 8$ and $\eta = \pi/4$. We illustrate the orbital evolution of planets c and d with the (x - η) diagram (see Fig. 4a) and with e_c and e_d as a function of time (see Fig. 4c). These results show that the planets’ orbits initially librate relative to each other. The planets remain on librating closed tracks in the (x - η) diagram after the disk is totally depleted. But, as a consequence of the secular-resonance passage, the eccentricity of planet c becomes smaller than that of the planet d. The time-averaged eccentricities after the disk depletion are $\langle e_c \rangle \simeq 0.12$ and $\langle e_d \rangle \simeq 0.2$.

We also consider a second set of initial conditions with $x = 8$ ($e_c = 0.4$, $e_d = 0.05$) and $\eta = 3\pi/2$. In this case, the planets’ orbits initially circulate relative to each other, but, they become trapped in librating orbits during the passage through the secular resonance (see Fig. 4b). The mean eccentricities after the total depletion of the disk are very similar to that obtained in the case of panel (a), because they are determined by the conservation of angular momentum (eq. [D6]).

We also carried out numerical integration of the full equations with the uniform-disk-

depletion prescription with $t_{\Delta N} = 10^5$ years, $r_{\text{edge}} = 4.5\text{AU}$. When the same initial condition is used (*i.e.* $x = 8$ and $\eta = \pi/4$) were used, the pattern of the orbital evolution with this prescription (see Fig. 5a) is not significantly changed from that in Figure 4a. In panels b and c, we show the evolution from $(x = 8, \eta = \pi)$ and $(x = 5.6, \eta = 0)$. The pair of planets in panel b has an initially wide open circulating track. During the disk depletion, they temporarily enter into closed librating track. But, their orbital configuration becomes wide open again when most of the disk material is depleted. The results of these numerical calculations show that as long as the depletion time scale of the disk is longer than the oscillation period of eccentricity, the planets' orbits evolve adiabatically. Those systems with librating orbits in $(x-\eta)$ diagram prior to the disk depletion usually remain on the closed librating tracks after disk is totally depleted despite large changes in magnitude of x as in the case of Ups And (see below). Those pairs of planets with the widely open circulating tracks initially generally remain on open circulating tracks after the disk depletion is completed as in the case of HD168443 (see below). Under some circumstances, it is also possible for planets with marginally circulating/librating initial orbits to undergo transition after the disk depletion.

4.2. Orbital Evolution of Circulating Planets Around HD168443

Next we consider the case of the planetary system around HD168443 for which we assume the mass ratio to be $M_b/M_c = 0.451$. Figure 6 shows the time evolution of the equi-Hamiltonian contour map of the HD168443 system. The nebula edge retreats from inside to outside (from panel 1 to panel 5). The secular resonance occurs when $\Delta N = -0.86$ with $r_{\text{edge}} = 7.2\text{AU}$. Similar to the case of the planetary system around Upsilon Andromeda, the librating orbit with $|\eta| < \pi/2$ are confined in regions with $e_b > e_c$ prior to disk depletion. But, in the case of HD168443 system, the domain of closed librating tracks is small. (In contrast, for small $M_b/M_c(a_b/a_c)^{1/2}$, the domain of open circulating tracks is large as is the case for planets c and d around Ups And). The domain of closed librating tracks with $|\eta| < \pi/2$ moves downward in the Hamiltonian map as disk depletion proceeds. If planets of HD168443 initially follow open circulating tracks prior to the disk depletion, they would remain on the open circulating tracks after the disk depletion. In this case, during the onset of secular resonance, planets b and c may briefly attain a librating track before moving onto an open circulating track as the disk continues to deplete. Throughout the epoch of disk depletion, the planets' longitudes of periastrons are widely separated such that little angular momentum may be exchanged between them. Consequently, the net change of eccentricities is limited.

Figures 7 show the numerically computed orbital evolution. The disk potential is calculated with the uniform depletion prescription in which we specify $t_{\Delta N} = 10^6$ years. Figures 7a and b represent the first model with $x = 6$ and $\eta = 0$ initially and Figures 7c and d show the second model with $x = 1$ and $\eta = 0$ initially. For the first model, the eccentricity of outer planet c becomes larger than that of planet b after the disk depletion in contrast to the observed eccentricities of planets b and c. With the initial x smaller than $\gamma_d^{-1/2}$, the results for the second model (in panel c) reproduce the present eccentricities of both planets. (For presentation simplicity, the notation of $\gamma_d = (a_b/a_c)^{1/2}(M_b/M_c)$ which represents planets b and c.) The extent of the open circulating track is large both before and after the disk depletion. During the passage through the secular resonance, the planets’ orbits are temporarily trapped in the libration cycles around $\eta = \pi$. But the two planets break free from their librational state to follow a circulation path after the disk is totally depleted.

4.3. Dependence on Disk Model

4.3.1. Single External Disks

The initial eccentricities of planets, prior to the disk depletion, can be inferred from the conservation of the total angular momentum and energy of the planets. We represent the mean eccentricities ($\langle e_c \rangle$ and $\langle e_d \rangle$) of the planets c and d around Ups And by their values near the libration center (*i.e.* with $x = x_m$ and $\eta = 0$). In Figure 8a, we plot the values of $\langle e_c \rangle$ and $\langle e_d \rangle$ for various Σ_0 and r_{edge} . The eccentricities $\langle e_c \rangle$ and $\langle e_d \rangle$ are shown by filled circle for six different pre-depletion disk surface densities ($5 \sin i$, $4 \sin i$, $3 \sin i$, $2 \sin i$, $1 \sin i$, and zero times that of the minimum mass model at r_{edge} where zero corresponds to the present state). The model with $k = 3/2$ has the same power-law index for the Σ distribution as that of the minimum mass nebula model so that these scaling factors for $\Sigma(r_{\text{edge}})$ also represent that for the disk mass.

We also adopt three different pre-depletion locations of the edge ($\log(r_{\text{edge}}/a_d) = 0.14, 0.2, 0.3$). The pre-depletion locations of the edge correspond to 3.53, 4.06, and 5.11 AU, respectively. The apogee distance of planet d ($a_d(1 + e_d)$) is unlikely to exceed the inner edge of the outer disk (r_{edge}) because its eccentricity may be effectively damped and the disk may be strongly perturbed (Papaloizou et al. 2001). From this requirement, we note that $r_{\text{edge}} > 3.5\text{AU}$ for the present value of $e'_d = 0.35$. Prior to the disk depletion, it is possible that e'_d may be close to zero. Nevertheless, the tidal torque of planet d can induce the formation of a gap with a width which is $\Delta r \sim \sqrt{12}R_{\text{Roche}}$ where $R_{\text{Roche}} = (M_d/3M_*)^{1/3}a_d \simeq 0.35a_d$ is its Roche radius (Bryden et al. 1999). Thus, we adopt the minimum value of $r_{\text{edge}} \simeq a_d + \Delta r \simeq 3.5\text{AU}$ (see top panel of Fig. 8a).

The solid line shows an ellipse which is delineated by the conservation of total angular momentum (see eq. [D6] in Appendix). To second order in eccentricity, the conservation of the total angular momentum (eq. [D4] in Appendix) implies that

$$\frac{e'_d{}^2 - e_d^2}{e'_c{}^2 - e_c^2} = \frac{M_c \sin i \sqrt{a_c}}{M_d \sin i \sqrt{a_d}} = \gamma_d, \quad (17)$$

where e'_c and e'_d are the pre-depletion eccentricities of planets c and d respectively. The value of $\gamma_d \sim 0.286$ in the case of planets around Ups And. A maximum value of $e'_d = 0.37$ is attained for a minimum value of $e'_c = 0$. But, our results in Figure 4 indicate that x decreases during the disk depletion so that $e'_c > e_c$ and the maximum value of e'_d is unattainable.

When the disk edge is relatively close to the planet (top panel), $e'_c > 0.65$ and $e'_d < 0.1$ if the pre-depletion disk mass is greater than $2 \sin i$ times that of the minimum mass nebula model. But for larger values of r_{edge} , the pre-depletion eccentricities approach their present values as the contribution of the disk mass to the total gravity becomes vanishingly small.

The secular resonance occurs at $x_m \sim 2$ in the case of Ups And. As long as there was the disk which corresponds to a pre-depletion $e_c > 0.51$, the planets pass through the secular resonance. Note that with an arbitrarily large disk mass, e'_d vanishes while e'_c attains a maximum value of 0.69. Even under these extreme condition, the orbits of the two planets do not cross and remain stable. During the disk depletion, the eccentricities of planet c and d coincide with each other at about 0.33. For the pre-depletion eccentricity of planet c to be > 0.33 (which is generally the case with the exception of the three least massive initial disk models), the inversion of eccentricity ratio between the planet c and d around Ups And occurs.

Because the influence of the disk on the planet is mainly due to the gas near the r_{disk} , the above results are insensitive to changes to the surface density distribution at large radii. In Figure 8b, we set $r_{\text{edge}} = 4.057\text{AU}$ ($\log(r_{\text{edge}}/a_d) = 0.2$) and considered three sets of Σ distributions with $k = 2$, $k = 1$, and $k = 1/2$ (Fig. 8b). We adopt six sets of values of the surface density $\Sigma(r_{\text{edge}})$ of each model at r_{edge} . For disk with similar surface density scaling factor, there are no significant differences between three panels. The detailed disk structure is not important for the evolution of the planetary eccentricities in our model.

4.3.2. Interplanetary Rings and Outer Disks

After the emergence of multiple planets, gap formation effectively cuts off gas flow from the external disk across the outermost planet's orbit. Since both dynamical and viscous time scales are rapidly increasing function of the disk radius, the disk interior to the gap

is depleted rapidly (Lin & Papaloizou 1986b). Due to a shepherding effect induced by the multiple planets (Goldreich & Tremaine 1979), the gaseous interplanetary rings may be preserved for a much longer time scale than the internal disk. Nevertheless, the dissipation of the competing tidal perturbations by the planets can lead to ring dispersal well before the depletion of the external disk (Bryden et al. 1999).

In the present context, the evolution of the eccentricity ratio (x_{m0}) at the libration center around $\eta = 0$ depends intricately on the depletion pattern of both the ring and disk as well as the locations of the edges of the ring and disk. For example, the value of x_{m0} is smaller for interplanetary rings with inner edge d_{in} closer to the inner planet. In contrast, the value of x_{m0} is larger for interplanetary rings with outer edge d_{out} closer to the outer planet. The balance between these effects determines the evolution of the eccentricity ratio. In order to illustrate these dependence, we consider the epoch when planets c and d around Ups And were surrounded by an interplanetary ring and an external disk. We adopt a surface density distribution which is $5 \times \sin i$ that of the minimum mass solar model. A hole is cut out interior to d_{in} . An annular strip is also removed between d_{out} and r_{edge} . By fixing the inner edge of the external disk to be $r_{\text{edge}} = 4$ AU, we compute the value of x_{m0} as a function of d_{in} (see Fig. 9). In these calculations, we used eight values of the outer edge of the ring d_{out} , ranging from 1.2 to 1.9 AU in intervals of 0.1AU.

The results in Figure 9 indicate that when $d_{\text{out}} < 1.66$ AU, the gravitational perturbation of the ring on the inner planet always surpasses that on the outer planet. Consequently, the value of x_{m0} is reduced below that ($x_{\text{disk}} \sim 12$) in the external-disk-only (*i.e.* ringless) models. In these small d_{out} cases, x_{m0} approaches to 12 for relatively large d_{in} as the ring’s influence weakens. But, in the limit $d_{\text{out}} > 1.66$ AU, x_{m0} becomes larger than x_{disk} for relatively large d_{in} . For example, when $d_{\text{out}} = 1.8$ AU, x_{m0} becomes larger than x_{disk} at $d_{\text{in}} > 1.5$ AU because the ring’s perturbation on the outer planet is enhanced. Also in this large d_{out} limit, x_{m0} becomes smaller than current observed eccentricity ratio of 0.66 at $d_{\text{in}} < 1.33$ AU. For all values of a_{out} , the pre-depletion values of x_{m0} in this model is always larger than the current observed eccentricity ratio.

In Figure 10, we show the evolution of equi-Hamiltonian contours in a model with both ring between planets c and d and an external disk beyond planet d. We adopt a prescription in which the ring is depleted uniformly prior to the uniform depletion of the external disk. For our model, we specify $\log(d_{\text{in}}/a_c) = \log(a_d/d_{\text{out}}) = 0.2$ for the ring and $\log(r_{\text{edge}}/a_d) = 0.2$ for the external disk. Our numerical results indicate that x_{m0} is initially smaller than current observed eccentricity ratio (panel 1). The ring proceeds to be depleted during the epochs represented by panels (2) and (3). When the ring mass is reduced to half of its original value, x_{m0} become ~ 2 (panel (2)), *i.e.* the system passes through a state of secular resonance. The

entire ring is depleted while the external disk is preserved during the epoch represented by panel (3). After that, the contours again evolve through a state of secular resonance (when 1/3 of the external disk is depleted in panel 4) to current values (in panel 5) as in the case of Figure 3.

Although the same pattern of evolution occurs in the case of planets around HD168443, there is little change in the eccentricities of either planets since the contour of their eccentricity ratio always retains the values around $\gamma_d^{-1/2}$. We realize that the evolution of the interplanetary ring is determined by the process of gap formation and planet-disk tidal interaction, its influence on the eccentricity evolution of the planets should be analyzed along with its non axisymmetric contributions. The results of such analyses will be presented elsewhere.

5. IMPLICATIONS ON THE PROTOPLANETS' ORBITAL ECCENTRICITY PRIOR TO THE DEPLETION OF THEIR NASCENT DISKS

5.1. Planets around Ups And

First, we consider the evolution of planets c and d around Ups And. We infer from their present librating orbits and the results in Figure 2 that these planets followed a close librating track prior to the disk depletion. Our results also indicate that when the disk dominated the planets' apsidal precession, the domain of close librating tracks with $|\eta| < \pi/2$ resided in the parameter region with $e_c > e_d$. Thus, the present observed librating orbits of planets c and d would be attainable if $e_c > e_d$ prior to the disk depletion. Since $e_c < e_d$ today, the passage through the secular resonance must have led to the inversion of this ratio. In Figure 11, we map out, in the $(x-\eta)$ plane, the most likely initial domain which may have led to the present planetary orbits in the Ups And system (panel a). The periapses of those pairs of planets which initially occupied region 1 maintain their near alignment despite the large changes in x during the disk depletion. These systems enter the domain of closed librating tracks in the $(x-\eta)$ plane after the disk is completely depleted. Their orbits become very similar to the present orbits of planets c and d. Planets in region 2 have open circulating tracks prior to the disk depletion. Their orbits remain on circulating tracks after the disk depletion. Among those pairs of planets which originated from both regions 1 and 2 ($x > \gamma_d^{-1/2} \sim 2$), the eccentricity ratio is reduced after the disk depletion. Thus, we infer those pairs of planets which currently occupy the region $x(= e_c/e_d) \lesssim 1$ are originated from the domain $x \gtrsim 2.5$ prior to the disk depletion. Those pairs of planets with $x < 2$ initially cannot attain the present observed values of $x(\sim 0.6)$ because the magnitude of their x increases during the

disk depletion.

In the absence of a strong non axisymmetric torque associated with the planet-disk interaction, secular interaction between the planets does not alter the total angular momentum and energy of the system. In contrast to the eccentricity ratio (x) between planets c and d, the magnitude of eccentricities cannot be excited by the sweeping secular resonances alone. The equation (17) indicates that if both planets had nearly circular orbits initially, their eccentricity would remain small after the disk is completely depleted. Thus, around Ups And, at least planet c must have acquired some initial eccentricity prior to the epoch of planet formation.

Up to now, we have neglected the effect of non axisymmetric torque associated with the planet-disk interaction. During their formation, the eccentricities of isolated protoplanets are damped and excited as a result of their interaction with their nascent disks at the corotation and Lindblad resonances respectively. For protoplanets with masses comparable to that of Jupiter, the damping effect of the corotation resonances is stronger than the excitation effect of the Lindblad resonances (Goldreich & Tremaine 1980). But protoplanets with masses an order of magnitude larger than that of Jupiter may open relatively wide gaps in protostellar disks. In this limit, the protoplanets' corotation resonances may be cleared of disk gas such that their eccentricity may be excited (Artymowicz 1993; Papaloizou, et al. 2001). For modest inclination angle between the their orbital plane and the line of sight, neither planet c nor d have sufficiently large mass to clear a wide gap. But, planet c is likely to form prior to planet d. The tidal torque of planet d may truncate the disk well beyond the region which contains any corotation resonance for planet c so that the latter's eccentricity is excited whereas that of planet d is damped.

The actual mass of planets c and d depends on the value of $\sin i$. If $i < 20^\circ$, the mass of planet d would be sufficiently large for its interaction with the disk to excite eccentricity. The constraint on the inclination angle inferred from the dynamical stability of the planetary system around Ups And indicate that $i > 12 - 45^\circ$ (Lissauer & Rivera 2001; Ito & Miyama 2001). In a multiple system, however, the rate of angular momentum transfer between planet d and the outer disk may be faster than that between it and planet c. We shall consider in a future contribution whether planet c will be able to attain a larger initial eccentricity.

It is also possible that the planets around Ups And was closer to each other in the past and dynamical instability may have led them to undergo orbit crossing (e.g., Chambers, Wetherill, & Boss 1996). Rasio et al. (1996) suggested that such a process may have led to the scattering of a planet close to the surface of its host star and subsequent tidal circularization may have caused it to become a short period planet. Around Ups And, regardless whether such a process can lead to the formation and survival of the short-period

planet b, planetary scattering may also have excited the eccentricity and modified the semi-major axes of both planets c and d (Weidenschilling & Marzari 1996, Lin & Ida 1997). During such encounters, planets with lower mass generally acquires larger eccentricity as a result of the conservation of the system’s total energy and angular momentum. Although these speculations provide arguments for planet c to have initially acquired more eccentricity than planet d, rigorous analysis is needed to quantitative verify these conjectures.

5.2. Planets around HD168443

In the case of planets around HD168443, the present orbit follows an open circulating track. In Figure 11b, we outline the necessary initial domain in the $(x-\eta)$ diagram, which would lead planets b and c to acquire their present orbital parameters. Planets which were initially in the region 2, would enter into open circulating tracks after their nascent disk is completely depleted. But their eccentricity ratio would not generally match those inferred from the observations of HD168443. The most likely initial domain of planets around HD168443 (with their current dynamical properties) is mapped out as region 1. During the passage through secular resonance, the eccentricity of planet c decreases while that of planet b increases slightly. The geometry of $(x-\eta)$ diagram is reversed during the passage through the secular resonances, *i.e.*, at the point $x = \gamma_d^{-1/2}$. This small change is due to the present value of x being close to that of $\gamma_d^{-1/2}$ in the HD168443 system. In contrast, present x of planets around Upsilon Andromeda is much smaller than $\gamma_d^{-1/2}$.

5.3. Other Multiple-planet Systems

We comment here about another system of planets around HD74156 (Table 1(c)). In this system, the outer planet is more massive than the inner planet. Since their orbits are circulating (similar to those of the planets around HD168443), the evolution of this system during the disk depletion would be very similar to that described in §4.2 for the planets around HD168443. However, the present value of x is not close to that of $\gamma_d^{-1/2}$. The inversion of the eccentricity ratio is expected to occur in the case of planets around HD74156 (similar to those of the planets around Ups And).

Our own solar system also contains multiple gaseous giant planets. In this case, the inner planet, Jupiter, is more massive than the outer planet, Saturn. Their longitudes of periastron are not aligned with each other. The ratio of the Jovian eccentricity to the Saturnian eccentricity (e_J/e_S) varies between the range of 0.3 and 5 with time. In this

case, the orbits of Jupiter and Saturn do not pass through the secular resonance during the depletion of the primordial solar nebula. Therefore, the initial orbits attained by Jupiter and Saturn during their formation would not be significantly changed as a consequence of the disk depletion. This evolution pattern is similar to that of the two-planet system around 47 UMa. Those two planets have masses 2.0 and 0.67 M_J and semi-major axes 2.1 AU and 3.8AU, respectively (Table 1(d)).

In general, those systems where the outer planets are more massive than the inner planets (such as the planetary systems around Ups And, HD168443, and HD74156), the depletion of the outer disks induces a secular resonance which sweeps through both planets. But in the opposite situation where the inner planets are more massive (more precisely, where $\gamma_d^{-1/2} < 1$) such as the planetary systems around the Sun and 47 UMa, the depletion of the disk does not lead to the secular resonances between the planets. Thus, the changes of the eccentricities are not so large. The planets around HD12661 (Table 1(e)) have librating orbits with $\eta \sim \pi$. During the disk depletion, the secular resonance passes through this system (*i.e.* x_m attains a value of $\gamma_d^{-1/2}$) because its $\gamma_d^{-1/2} > 1$ (the inner planet is massive than the outer planet). Today, the value of x_m around the libration centers at π is slightly larger than $\gamma_d^{-1/2}$. Thus, the pre-depletion value of x_m must be smaller than $\gamma_d^{-1/2}$. Nevertheless, the magnitude of the eccentricity change is relatively small because the present value of x_m is close to that of $\gamma_d^{-1/2}$.

6. SUMMARY AND DISCUSSIONS

In this paper, we consider the secular interaction between pairs of coplanar planets. Provided these planets are not locked in a mean motion resonance, their secular interaction leads to angular momentum exchange without energy transfer between them. Consequently, both planets undergo apsidal precession and eccentricity modulation about some mean values. Thus, dynamical evolution of these systems of planets is best illustrated by the ratio of their eccentricity x and the relative longitude of their periastrons η . For example, based on their observed orbital elements, we find that gravitational perturbation between the outer two planets around Ups And causes both η and x to modulate, with small amplitude, along a close librating track around $\eta = 0$ and $x \sim 0.66$ (see Fig. 1).

Although the mean eccentricities of these planets are constant today, they may have undergone significant changes during the epoch when their nascent disks were depleted. In order to extrapolate the initial dynamical properties of planetary systems, we consider the precession caused by the self gravity of these disks. We show that contribution from the disks initially dominates the precession frequency of the planets and regulates the angular

momentum exchange rate between them. As their influence fades during the disks’ depletion, the precession eigenfrequencies of the planets’ longitude of periastron pass through a state of secular resonance.

As a result of this transition, the magnitude of both planets’ eccentricities changes with their ratio inverted. But, provided the disk depletion proceeds on a time scale long compared with the precession frequencies associated with the secular interaction between the planets, the libration amplitude of η is not significantly changed due to the preservation of an adiabatic invariance. Thus, if a pair of planets started out with a close librating orbit prior to the disk depletion, they would generally retain the librating nature of their secular interaction after the disk depletion. Planets with open circulating tracks initially would generally evolve to attain other open circulating tracks after the disk depletion. However, the circulating track may temporarily enter into closed librating track near the secular resonance. Planets with marginally circulating orbits (close to librating orbits) prior to the disk depletion may sometimes attain librating orbits after the disk depletion provided the difference between the libration and resonant centers (*i.e.* $|x_m - \gamma_d^{-1/2}|$) is reduced during the transition. Inversely, planets with marginally librating orbits prior to the disk depletion may also sometimes attain circulating orbits after the disk depletion provided the difference between the libration and resonant centers is increased.

Using these results we infer the kinematic properties of planetary systems around both Ups And and HD168443. During the passage of the secular resonances, the libration time scales of the planets around these two stars are 2×10^4 and 10^5 years, respectively. Provided the external axisymmetric disk is depleted on a time scale longer than these libration time scales, transition through the secular resonance is adiabatic.

In this contribution, we show how the process of disk depletion may lead to significant modifications in the eccentricity distribution within some extrasolar multiple planetary systems. These changes are the result of secular perturbation the planets exerted on each other. But planetary secular perturbation and the axisymmetric potential of evolving disks alone do not lead to eccentricity excitation. We have not quantitatively addressed the issue of initial eccentricity excitation among isolated planets or at least one planet in a multiple planetary system. We will discuss these problems in the future.

MN would like to thank R. Mardling for her helpful suggestions. MN used the parallel computer (Silicon Graphics Origin 2000) of Earthquake Information Center of Earthquake Research Institute, University of Tokyo. This work was partly performed while MN held a National Research Council Associateship at NASA Ames. This work is supported in part by NASA through grant NAG5-10727 and NSF through AST-9987417 to D. N. C. L..

A. PRECESSION DUE TO THE DISKS' GRAVITY

In this section, we evaluate ΔN in equation (9). After protoplanets have acquired a sufficiently large mass, they induce the formation of a gap near the orbit through tidal interaction with the disk (Goldreich & Tremaine 1980; Lin & Papaloizou 1980, 1993). While the disk material can no longer be rapidly accreted onto the protoplanet (Bryden et al. 1999), it continues to contribute to the gravitational potential. Although the disk does not have a sufficiently large mass to modify the angular frequency of the planet's orbit, its gravity can induce precession (Ward 1981). The disk's contribution to the gravitational force in the radial direction at r is

$$F_r(r) = -\frac{d\Psi}{dr} = -2G \int_0^\infty y \Sigma(y) \left(\frac{E(\psi)}{1-y} + \frac{K(\psi)}{1+y} \right) dy, \quad (\text{A1})$$

where Σ is the surface density of the disk, Ψ is the potential, $y \equiv r'/r$, $\psi \equiv 2y^{1/2}/(1+y)$, $K(\psi)$ and $E(\psi)$ are elliptic integrals of first and second kind, and G is the gravitational constant (eq. 2-146 in Binney & Tremaine 1987). The associated precession frequencies for planets c and d can be obtained from

$$N_{c,d} = (\Omega_{c,d} - \kappa_{c,d})t_c = \frac{n_{c,d}t_c}{2GM_*} \left(\frac{\partial}{\partial r} r^3 F_r \right)_{r=a_{c,d}}, \quad (\text{A2})$$

where $\Omega_{c,d}$ and $\kappa_{c,d}$ are respectively the angular and epicycle frequencies at semi-major axis of planets c and d ($a_{c,d}$). Depending on the Σ distribution, $N_{c,d} \sim O(n_{c,d}t_c M_D/M_*)$ where $M_D = \Sigma a_{c,d}^2$ is the characteristic disk mass at $r = a_{c,d}$ respectively. From equation (A2), we find

$$\Delta N = N_c - N_d = \frac{t_c}{2GM_*} \left(n_c \left(\frac{\partial}{\partial r} r^3 F_r \right)_{r=a_c} - n_d \left(\frac{\partial}{\partial r} r^3 F_r \right)_{r=a_d} \right), \quad (\text{A3})$$

with its sign determined by the Σ distribution. For disks with finite Σ only outside the planets' orbit, the addition of the disk self gravity leads to both N_c and N_d to be positive. Since planet d is closer to the external disk, $N_d > N_c$ so that ΔN is negative. For disks which engulf both planets' orbits, ΔN can still be negative provide Σ does not decrease too rapidly with r . For example, if we use the minimum mass nebula model (Hayashi et al. 1985) as a fiducial prescription for Σ such that

$$\Sigma = 1.7 \times 10^3 (r/1\text{AU})^{-1.5} \text{gcm}^{-2}, \quad (\text{A4})$$

ΔN is negative.

B. ORBITS OF LIBRATING AND CIRCULATING PLANETS

Using linearized equations (8) and (9), we consider here three families of orbits in systems which contain two planets. We assume that the two planets orbit on the same plane as the disk.

B.1. The Orbits of Librating Planets

As an example, we consider the planets c and d around Ups And. For planets c and d around Ups And, $C = -0.4$, $\gamma_d = 0.29$. The longitudes of these two planets are aligned such that their $\eta \simeq 0$ today. The present values of $x = 0.66$ and $t_c = 1.1 \times 10^3$ years. With these values, we show below that secular interaction between the two planets induces x and η to undergo small amplitude oscillation around stationary points. These points correspond to extrema for x and η . From the linearized equations (8) and (9) of secular motion, we find that these extrema occurs at $\eta = 0$ and π .

For $\eta = 0$, a stationary solution can be obtained for $x = x_m (> 0)$ where x_m is a root of the quadratic equation

$$x_m^2 - \left(\frac{\Delta N + 1 - \gamma_d}{\gamma_d C} \right) x_m - \frac{1}{\gamma_d} = 0. \quad (\text{B1})$$

With $x = x_m$ and $\eta = 0$, longitudes of the periape of both planets are aligned and precess together, even though $g_1 \neq g_2$. Consequently, there is no angular momentum exchange and the eccentricities of both planets are conserved. For solutions near the stationary point with $\eta = \pi$, x_m can be obtained from a similar equation where

$$x_m^2 + \left(\frac{\Delta N + 1 - \gamma_d}{\gamma_d C} \right) x_m - \frac{1}{\gamma_d} = 0. \quad (\text{B2})$$

In the $(x-\eta)$ diagram, these orbits follow the equi Hamiltonian contours (see Appendix D). Angular momentum is being continually exchanged between the planets, leading to an eccentricity modulation. However, the libration is centered around $\eta = 0$ or $\pm\pi$ where there is no net torque between the two planets. Although the range of η modulation ($\Delta\eta$) is limited, the two planets are *not* in the center of secular resonance because η modulates with a frequency ω which does not vanish with arbitrarily small $\Delta\eta$.

We now consider a small perturbation about the stationary point. For small values of η and $\epsilon \equiv x/x_m - 1$, equations (8) and (9) can be linearized in η and ϵ such that

$$\frac{d\epsilon}{d\tau} = \frac{C}{x_m} (1 + \gamma_d x_m^2) \eta, \quad (\text{B3})$$

$$\frac{d\eta}{d\tau} = -\frac{C}{x_m}(1 + \gamma_d x_m^2)\epsilon. \quad (\text{B4})$$

Combining these two equations, we find the solution

$$\epsilon = \epsilon_0 \sin(\omega\tau), \quad \eta = \eta_0 \cos(\omega\tau), \quad \text{with} \quad \eta_0 = \pm\epsilon_0, \quad (\text{B5})$$

where the oscillation frequency is

$$\omega = \frac{\pm C}{x_m} (1 + \gamma_d x_m^2), \quad (\text{B6})$$

where the signs of the expression for η_0 and ω are the same. Near the stationary point $x = x_m$ and $\eta = 0$, ω is also approximately the difference of the precession frequencies of the two planets because ϖ for both precess in the same direction.

B.2. Orbit of Circulating Planets

As another example, we use the planets around HD168443. For planets b and c around HD168443, $C = -0.13$, $\gamma_d = 0.14$, and $t_c = 1.9 \times 10^3$ years. For notational consistency, we use the subscription for the inner planet is c and that for the outer planet is d . With these parameters, $\Delta N = 0$ for $x_m = 0.15$ (or 46) and $\eta = 0$ (or π). The observed value of $x = 2.65$ and $\eta = 1.92$ which is far from the stationary point $x = x_m$ and $\eta = 0$ (or π). With these parameters, $|A_1| \gg |A_2|$ (see eqs. [7] and [9]), we expect the orbits of planets b and c to circulate with respect to each other. In this case, the linearized equations (B3) and (B4) are no longer applicable. The small magnitude of C in equation (8) implies that the modulation amplitude of x is small compared with its average value. The dominance of the term of $1 - \gamma_d + \Delta N$ in equation (9) implies that, to zeroth order in τ , $x \simeq x_0$ and $\eta \simeq (1 - \gamma_d)\tau$ where x_0 is a constant. Expansion to the next order in τ yields the solution that

$$\eta \simeq (1 - \gamma_d + \Delta N)\tau + \frac{C}{x_0} \frac{(1 - \gamma_d x_0^2)}{(1 - \gamma_d + \Delta N)} \sin(1 - \gamma_d + \Delta N)\tau, \quad (\text{B7})$$

$$x \simeq x_0 - \frac{C}{1 - \gamma_d + \Delta N} \cos(1 - \gamma_d + \Delta N)\tau, \quad (\text{B8})$$

so that the circulation period is $t_l \simeq 2\pi t_c / (1 - \gamma_d + \Delta N) \sim 1.4 \times 10^4$ years for $\Delta N = 0$.

B.3. Non Periodic Orbits Near Secular Resonance

In addition to the librating and circulating orbits, there is another family of non periodic orbits for the case when $|A_1| \leq |A_2|$. In the limit that both x and η have values which are

very different from x_m and $\eta=0$ (or π), η would evolve rapidly to a phase angle

$$\eta_1 \simeq \cos^{-1} \left(-\frac{A_1}{A_2} \right) = \cos^{-1} \left(\frac{-A_1 x}{C(1 - \gamma_d x^2)} \right), \quad (\text{B9})$$

such that $d\eta/d\tau$ is, to within the first order approximation, reduced to zero (see eq. [9]) and the two planets become phase locked. Within the same order approximation, x becomes x_1 and the evolution of x is determined by

$$\frac{dx}{d\tau} = \frac{dx_1}{d\tau} \simeq C(1 + \gamma_d x_1^2) \sin \eta_1 \simeq \pm C(1 + \gamma_d x_1^2) \left(1 - \frac{A_1^2 x_1^2}{C^2(1 - \gamma_d x_1^2)^2} \right)^{1/2}, \quad (\text{B10})$$

provided $|A_1|$ remains smaller than $|A_2|$. (In Appendix C, we consider the depletion of the disk during which the magnitude of A_1 evolves with time.)

The plus and minus signs on the right hand side of equation (B10) correspond to $0 \leq \eta_1 \leq \pi$ and $\pi \leq \eta_1 \leq 2\pi$ respectively. Increases/decreases in x are equivalent to eccentricity excitation/damping for body c. As a consequence of x evolution, η also adjust to $\sim \eta_1$ such that the evolution of the planets' orbit is non periodic. Nevertheless, during the raise/decline in x , the two planets may also undergo small amplitude (x_2, η_2) libration around the evolving guiding center at x_1 and η_1 . The evolution of x_2 and η_2 can be determined from the next order expansion of equations (8) and (9) such that

$$\frac{dx_2}{d\tau} = B_1 \eta_2 + B_2 x_2, \quad (\text{B11})$$

$$\frac{d\eta_2}{d\tau} = B_o(\tau - \tau_0) + B_3 x_2 + B_4 \eta_2. \quad (\text{B12})$$

The coefficients are

$$\begin{aligned} B_0 &= \Delta \dot{N}, & B_1 &= C(1 + \gamma_d x_1^2) \cos \eta_1, \\ B_2 &= 2C\gamma_d x_1 \sin \eta_1, & B_3 &= -(C/x_1^2)(1 + \gamma_d x_1^2) \cos \eta_1, \\ B_4 &= -(C/x_1)(1 - \gamma_d x_1^2) \sin \eta_1, \end{aligned} \quad (\text{B13})$$

where $\Delta \dot{N} = d\Delta N/d\tau$ and the fiducial dimensionless time τ_0 corresponds to the instance when the two planets first enter into a phase lock, *i.e.* when their $x = x_1$ and $\eta = \eta_1$. The solution of equations (B11) and (B12) can be expressed as

$$\begin{aligned} x_2 &= x_{20} \exp\{\omega_{20}(\tau - \tau_0)\} + x_{21} \exp\{\omega_{21}(\tau - \tau_0)\} + B_5 \tau + B_6, \\ \eta_2 &= \frac{1}{B_1} [(\omega_{20} - B_2)x_{20} \exp\omega_{20}(\tau - \tau_0) + (\omega_{21} - B_2)x_{21} \exp\omega_{21}(\tau - \tau_0)] \\ &\quad + \frac{1}{B_1} [B_5(1 - B_2\tau) - B_2 B_6], \end{aligned} \quad (\text{B14})$$

where x_{20} and x_{21} are the amplitudes of oscillations and

$$B_5 \equiv \frac{B_0 B_1}{B_2 B_4 - B_1 B_3} \quad \text{and} \quad B_6 \equiv \frac{(B_2 + B_4) B_5 - B_0 B_1 \tau_0}{B_2 B_4 - B_1 B_3}, \quad (\text{B15})$$

with the growth rate

$$\omega_2 = \omega_{20,21} = \frac{C}{2x_1} \{ (3\gamma_d x_1^2 - 1) \sin \eta_1 \pm (1 + \gamma_d x_1^2) (5 \sin^2 \eta_1 - 4)^{1/2} \}. \quad (\text{B16})$$

Note that when η_1 pass through the value $\sin^{-1}(4/\sqrt{5})$, $\omega_{20} = \omega_{21}$ and the solution of equations (B11) and (B12) becomes slightly modified from that in equations (B14). Also note that for $\eta_1 = 0$ or π , so that equations (B11) and (B12) reduce to equations (B3) and (B4) respectively. Also, ω_2 becomes purely imaginary ($\pm i\omega$) so all the orbits undergo libration about the stationary point. But, for a more general value of η_1 , ω_2 is complex, and oscillations about the evolving x_1 values either grow or decay depending on the value of η_1 . At the center of resonance where $A_1 = 0$ and $\eta_1 = \pi/2$ so that $\omega_2 = 2C\gamma_d x_1$ or $(C/x_1)(\gamma_d x_1^2 - 1)$. Both roots are real so that the x_2 either converge or diverge (if $x_1 > \gamma^{-1/2}$) without any oscillation. Note that oscillation about x_1 and η_1 only occurs if the magnitude of ω_2 is larger than B_5 such that changes in ΔN and x_1 occur in an adiabatic manner. For further discussions on the evolution of planetary orbits during the epoch of disk depletion, see Appendix C.

C. THE EVOLUTION OF MULTIPLE-PLANET SYSTEMS DURING THE EPOCH OF DISK DEPLETION

During the depletion of the disk, changes in the magnitude of ΔN can cause A_1 to change sign. In §4, we presented numerical results of orbital evolution during the epoch of disk depletion. Here, we present analytical solutions to interpret the numerical results. Following the discussions in Appendix B, we consider three initial orbits separately.

C.1. The Evolution of Two-Planet Systems with Initially Librating Orbits

In Appendix B.1, we show that the condition for libration is $|A_1| \leq |A_2|$ and $\epsilon_0 \ll 1$. For planets c and d around Ups And, $\Delta N = 0$ today so that $x_m \sim -C/(1 - \gamma_d) \sim 0.5$ and $\omega \sim 0.83$. Since the observed values of x and η are close to those of x_m and 0 respectively, the small-amplitude oscillator approximation is valid. The necessary condition for libration, *i.e.* $|A_1| \leq |A_2|$ is marginally satisfied. From equation (12), we find that the time scale for one complete libration cycle today is $t_l = \tau_{\text{lib}} t_c = 2\pi t_c / \omega = 8.5 \times 10^3$ years.

Prior to its depletion, five times minimum mass nebula model would lead to $M_D/M_d = \Sigma(a_d)a_d^2/M_d \sim 0.015$ and $\Delta N \sim -1.4$ (eqs. [A3] and [D2]). In this case, the necessary condition for libration is also marginally satisfied and it is possible to find a real positive solution to the quadratic equation (B1). Around the stationary point $x_m \sim 6.5$, there are also solutions which correspond small amplitude libration between planets c and d ($|\eta| \lesssim \pi/2$) despite the rapid precession induced by the disk's self gravity. The corresponding $\omega \sim 0.80$ for such a protoplanetary system is very similar to the present disk-free value of x_m .

During the depletion of the protostellar disk, the magnitude of ΔN gradually vanishes so that both x_m and ω changes with time. For $-1.5 < \Delta N < 0$, the condition for libration ($|A_1| \leq |A_2|$) is satisfied. Provide $\tau_{\text{lib}} < \tau_{A_1}$, $\tau_{\text{lib}} < \tau_\omega$, and $\tau_{\text{lib}} < \tau_{x_m}$ where

$$\tau_{\text{lib}} \equiv \frac{2\pi}{\omega} = \frac{2\pi x}{C(1 + \gamma_d x^2)}, \quad \tau_{A_1} \equiv \frac{A_1}{\dot{A}_1} = \frac{1 - \gamma_d + \Delta N}{\Delta \dot{N}}, \quad (\text{C1})$$

$$\tau_{x_m} \equiv \frac{x_m}{\dot{x}_m} = - \left(\frac{1 + \gamma_d x_m^2}{1 - \gamma_d x_m^2} \right) \tau_{A_1}, \quad \tau_\omega \equiv \frac{\omega}{\dot{\omega}} = \left(\frac{1 + \gamma_d x_m^2}{1 - \gamma_d x_m^2} \right)^2 \tau_{A_1}, \quad (\text{C2})$$

the libration of the planets' orbits is preserved while the librational center and frequency evolves adiabatically.

At the special phase when $A_1 = 0$, the second term in equations (B1) and (B2) reduces to zero and the stationary points with $\eta = 0$ and $\eta = \pi$ coincide with each other with $x_m = \gamma_d^{-1/2}$. We refer to this special configuration as librational degeneracy. In this state, all orbits librate either around $x_m = \gamma_d^{-1/2}$, $\eta = 0$ or π with two separatrix located on the $\eta = \pi/2$ and $3\pi/2$ (see Hamiltonian contours maps). From equation (6), we note that in this degenerate state, Δg_{12} attains a minimum value with respect to variations in ΔN . The oscillation frequency around the stationary points ω attains a minimum magnitude $2\gamma_d^{1/2}C$ with $x_m = \gamma_d^{-1/2}$ (see eq. [12]) which is ~ 1.8 for planets c and d around Ups And.

Note that in this state of librational degeneracy, $g_1 \neq g_2$ in general. However, if planet c has negligible mass, Δg_{12} would vanish and it would enter into a state of exact secular resonance and x_m would diverge. This asymptotic state represent the eccentricity excitation of asteroids by the Jovian planets. For finite values of γ_d , this state of librational degeneracy can also be considered as a state of secular resonance despite the finite value of Δg_{12} . The secular interaction between the planets forces them to librate so that their relative longitude of periaapse passage is confined to a limited amplitude.

We now consider the evolution of the librational amplitude. The action associated with the simple oscillator equations (B3) and (B4)

$$J = \int \dot{\epsilon} d\epsilon = \epsilon_0^2 \omega \int_0^{2\pi} \cos^2 \theta d\theta = \pi \epsilon_0^2 \omega \quad (\text{C3})$$

is invariant to first order in $\tau_{\text{lib}}/\tau_{A_1}$ or $\tau_{\text{lib}}/\tau_\omega$ (Goldstein 1980), which ever is larger. (For values of τ_{A_1} and τ_ω , see eqs. [C1] and [C2]). Based on this invariance, we can also determine the changes in ϵ_0 which is $\propto \omega^{-1/2}$. For planets c and d around Ups And, we adopted a model in which $\omega \sim 0.8$ both during the embedded phases and after the disk is completely depleted. Thus, we expect both ϵ_0 and η_0 to be remain invariant despite large changes in x_m . The numerical results in §4.1 is in agreement with this analytic derivation.

But, the condition for adiabatic evolution may not always be satisfied especially when the two planets pass through a phase of secular resonance with $x_m = \gamma_d^{-1/2}$ when the libration period takes the maximum value $t_l = -\pi t_c / (C\gamma_d^{1/2}) = 1.7 \times 10^4$ years and ω attains a minimum value of $\pm 2C\gamma^{1/2} = \mp 0.43$ (compared with its initial value of ~ 0.8). During this phase, the libration time scale τ_{lib} reaches a maximum. Although at the center of secular resonance, τ_{A_1} vanishes with A_1 , the more appropriate value for it is $\sim \Delta N / \Delta \dot{N}$ which remains finite. Nevertheless, it is possible for τ_{lib} to be larger than τ_{A_1} . Note that τ_{x_m} reduces to $\simeq \pm 2 / \Delta \dot{N}$ in the resonance. In accordance with equation (C2), τ_ω diverges. But, the characteristic time scale for ω evolution based on a second order expansion remains finite. The numerical results in §4.1 show a slight increase in ϵ_0 with a $\sim 6\%$ reduction in η_0 . In contrast, a 40 % increase in ϵ_0 is inferred from equation (C3). Nevertheless, for planets c and d around Ups And, the duration of non adiabatic evolution is brief so that the small amplitude libration around $x = x_m$ and $\eta = 0$ is preserved despite the large net changes in the magnitude of x_m .

Note that we have only consider the axisymmetric contribution of the disk to the total potential. Therefore the total angular momentum of the two planets is conserved during the disk depletion even though there is a net transfer of angular momentum between them which leads to the decline in e_c and the growth in e_d .

C.2. The Evolution of Two-Planet Systems with Initially Circulating Orbits 1: Asteroids

We now consider the orbital evolution of multiple-planet with initial values of $|A_1| \geq |A_2|$. In Appendix B.2, we showed that these systems have initially circulating orbits. There are two possible branches of solutions. First, we consider the limiting case of small γ_d ($\ll x^{-2}$) which is appropriate in the context of secular interaction between the asteroids and Jupiter for which $M_c \ll M_d$.

During the epoch of disk depletion, as the magnitude of A_1 in equation (9) is reduced below that of A_2 , η evolves to η_1 (see eq. [B9]) which reduces to $\eta_1 = \cos^{-1}(-A_1 x / C)$ in the

limit $\gamma_d \ll x^{-2}$. Since A_1 , A_2 , and C are negative, $\eta_1 = \pi$ when the planets first enter into a secular resonance. Also, equation (B10) implies that x_1 decreases/increases for η_1 slightly less/greater than π .

Let us first consider the case that η_1 is slightly less than π . Continual decline in x is attainable provided $d\eta_1/d\tau \leq 0$. The reduction in x leads to an increase in the magnitude of A_2 while the disk depletion causes a decrease in that of A_1 . Consequently, the magnitude of A_1/A_2 decreases in equation (B9), leading to a reduction in η_1 . This state of phase lock can only be maintained if η can adjust to η_1 and decrease to $\sim \pi/2$. So long this state of resonant phase locking is maintained, the magnitude of x (*i.e.* x_1) can decrease indefinitely. When A_1 passes through the zero value and becomes positive, x continues to decline. If the magnitude of x cannot be reduced as fast as that of ΔN , $|A_1| > |A_2|$ and the planets would attain circulating orbits. Even in the limit that the magnitude of x can be reduced as fast as that of ΔN , the planets are unlikely to attain librating orbits because their $\eta_1 \sim \pi/2$. Eventually, η_1 terminates its evolution with values slightly less than $\pi/2$ while the orbits of the massless particles are approximately circularized.

If the planets enter into the secular resonance with η slightly larger than π , x would increase. Further excitation of x requires $d\eta_1/d\tau \geq 0$. In equation (9), the growth in x reduces the magnitude of A_2 while that of A_1 is also decreasing. Phase lock can only be maintained if $|A_1| < |A_2|$ such that x cannot grow faster than $C/A_1 \simeq C/(1 - \Delta N)$ during the epoch of disk depletion. If x grows slower than C/A_1 , $d\eta/d\tau > 0$ and η_1 would increase to enhance the x growth rate. The magnitude of η_1 is determined by the ratio of A_1 and A_2 (see eq. [B9]). The evolution time scale of A_2 equals to τ_{x_m} . Equations (C1) and (C2) imply that $\tau_{A_1} \simeq \tau_{x_m}$ in the limit of small $\gamma_d x^2$. Thus, magnitude of A_1/A_2 is regulated to be less than unity as phase lock causes x to increase (see eq. [B10]).

As the resonant condition $1 - \Delta N \simeq 0$ is approached, η_1 increases to $3\pi/2$ and x grows at a maximum rate $dx/d\tau = -C$. So long this state of resonant phase locking is maintained, the magnitude of x can increase indefinitely. On the resonance, $g_1 = g_2$ such that the growth occurs regardless of the value η . Increases in x is equivalent to eccentricity excitation for the less massive body c . When A_1 passes through the zero value and becomes positive, x can have a sufficiently large value such that e_c may approach and even exceed unity. This eccentricity excitation process has been noted by Heppenheimer (1980) as a potential cause for the existence of highly eccentric asteroids.

As x increases in the resonances, there are three eventual outcomes: a) x becomes sufficiently large for e_c to exceed unity and body c to escape, b) the planets would attain circulating orbits as the magnitude of A_1 exceeds that of A_2 after $|\Delta N|$ decreases below ~ 1 if τ_{A_1} becomes much smaller than τ_{x_1} , and c) in systems with finite γ_d , the above

approximation become inappropriate when x exceeds $\gamma_d^{-1/2}$ (see below).

C.3. The Evolution of Two-Planet Systems with Initially Circulating Orbits 2: Two Planets with Comparable Masses

We now consider the second branch of solutions in which γ_d is finite. These parameters are more appropriate for the extrasolar multiple-planet systems in which the masses of the planets are comparable. The main difference introduced by the finite value of γ_d is the possibility of a transition as the value of x passes through $\gamma_d^{-1/2}$. This branch of solution is applicable for planets b and c around HD168443. We use the analytic solutions in this subsection to study the numerical results in §4.

For planets b and c around HD168443, $C = -0.13$, $\gamma_d = 0.13$, and $t_c = 1.9 \times 10^3$ years. In this system, the value of x_m depends sensitively on ΔN due to the small magnitude of C and γ_d . Within the uncertainty of analytic estimate, we estimate $M_D/M_d \sim 0.007$ and $\Delta N \simeq -4$ for five times minimum mass nebula model. Despite this relatively small value of $M_D (< M_d < M_*)$, the corresponding $x_m \simeq 180$. At this initial stage, $|A_1| > |A_2|$ and the planets follow circulating orbits which is well approximated by equations (B7) and (B8).

But, during the depletion of the disk, the decline of Σ reduces the magnitude of ΔN which passes through a stage of secular resonance in which $\Delta N \simeq \gamma_d - 1 = -0.86$ with the corresponding value of $x_m \simeq \gamma_d^{-1/2} = 2.6$ similar to the present value of x . In this limit, $|A_1| < |A_2|$ and the leading-order approximation with the solutions in equations (B7) and (B8) are no longer valid. Since the planets' orbits circulate relative to each other prior to entering this stage, the small-oscillation-amplitude approximation which led to the solutions in equation (B5) may also be inappropriate. Nevertheless, when the planets first enter into the resonance, $|A_1| = |A_2|$, $\eta_1 = \pi$, and ω_2 in equation (B16) becomes purely imaginary. The discussions in §B.3 indicates that during the passage through the resonance, all orbits are librating regardless of the amplitude of the libration cycles.

Within the resonance where $|A_1| < |A_2|$, the two planets become phase locked such that x_1 and η_1 evolve in accordance to equations (B9) and (B10). Depending on the rate of disk depletion, there are three potential outcomes for passage through the secular resonance. 1) In the limit that $\tau_{A_1} < \tau_{\text{lib}}$, the system evolves in an impulsive manner. Such a situation is relevant for rapid clearing of disks which contain long-period, low-mass, widely-separated planets with large t_c . In this case, there is insufficient time for the longitude of periapse to significantly circulate before the effect of secular resonance fades with the rapid disk depletion. During this rapid passage through the secular resonance, both x and η essentially retain

the values they had when they first entered into the resonance (x_1 and η_1). These values of η_1 and x_1 become the initial values of circulating orbits in the new disk-free potential. Since η_1 and x_1 are random parameters, the actual variational amplitude of the circulating orbits are unpredictable.

2) For systems such as planets b and c around HD168443, $\tau_{A_1} < \tau_{\text{lib}}$ so that the planets adiabatically evolve into a phase lock. The relevant governing equations become equations (B9) and (B10). In contrast to the case for the massless asteroids, the system first enters or finally exits the secular resonances with $\eta = 0$ if $x > \gamma_d^{-1/2}$ or π if $x < \gamma_d^{-1/2}$. In the middle of the resonant zone where $\gamma_d - 1 - \Delta N = 0$, although $x_m = \gamma_d^{-1/2}$, x generally does not equal x_m so that $\eta = \pm\pi/2$. (Even in the limit that $x = x_m$ at the center of resonances, A_1/A_2 also vanishes at the center of the resonance). Our analysis in §B.3 indicates that, at the center of resonance, both roots of $\omega_2 (= 2C\gamma_d x_1$ or $(C/x_1)(1 - \gamma_d x_1^2)$) are real so the amplitude of small perturbations either converge or diverge (if $x_1 > \gamma_d^{-1/2}$) from the stationary points without any oscillation. Note that in contrast to the case of massless asteroids, ω_2 changes sign as x_1 passes through $\gamma_d^{-1/2}$ so the system can neither be damped nor be excited indefinitely. This sign reversal of ω_2 limits the amount of changes in x_1 . Physically, this limit is due to the comparable momentum of inertia carried by planets of similar masses. In such systems, the exchange of angular momentum cannot lead to vastly different eccentricity changes for the two planets.

After passing through the center of the resonance, η_1 continues to evolve towards 0 or π in accordance to equation (B9) while x_1 evolves in accordance to equation (B10). When, η_1 reduces below $\sin^{-1}0.8$, ω_1 once again become complex and libration around x_1 and η_1 would resume if the magnitude of ω_2 is larger than B_5 such that changes in ΔN and x_1 occur in an adiabatic manner. But in equation (B15), the magnitude of B_5 is determined by $\Delta \dot{N}$ or equivalently τ_{A_1} . Thus, in the modestly rapid depletion case where $\tau_{A_1} \leq \omega_2^{-1}$, the difference between x_1 and x_m at the center of resonance is preserved. For small C magnitude (as in the case of HD168442), the width of the libration is small and x_m is also not changed significantly during the passage through the resonance. Thus, planets would not be able to enter into a librating state and the circulation pattern of their orbits is retained.

3) Finally, in the slow depletion limit where $t_{A_1} > \omega_2^{-1}$, the protracted passage through the secular resonance can greatly modify both x and η . As the planets exit the resonance, they can become trapped onto librating orbits. Large changes in x implies that at least one planet attains a relatively large eccentricity. In relatively compact multiple-planet systems, large eccentricity can cause mean motion resonances to overlap and dynamical instability. We shall address the issue of dynamical instability elsewhere.

D. HAMILTONIAN CONTOURS

These phase space evolution of the planets' orbits may be compared with equi-Hamiltonian contour maps. By expanding the disk potential in equation (14) for planets with eccentric orbits and then averaging it over their orbital period, Ward (1981) obtained the disturbing function due to the disk potential as follows:

$$\langle R_{\text{disk}} \rangle_{c,d} = e_{c,d}^2 \cdot \pi G \Sigma_0 a_{c,d} \left(\frac{a_0}{a_{c,d}} \right)^k \sum_{n=1}^{\infty} A_n \frac{n(2n+1)}{2n+k-1} \left(\frac{a_{c,d}}{r_{\text{edge}}} \right)^{2n+k-1} \equiv e_{c,d}^2 T_{c,d}. \quad (\text{D1})$$

Using this potential, ΔN of equation (A3) can be written as

$$\Delta N = \frac{8a_d^2}{Ga_c b_{3/2}^{(1)}} \left(T_c - T_d \left(\frac{a_c}{a_d} \right)^{1/2} \right). \quad (\text{D2})$$

When the disk depletion time scale is longer than characteristic librational time scale associated with equations (8) and (9) (time scales are given in Appendix C), ΔN can be regarded as quasi static. In this limit, the planets' orbits follow a single trajectory on $(x-\eta)$ plane depending on the magnitude of their Hamiltonian and angular momentum. Unless the orbits of the interacting planets are locked in mean motion resonances, the orbital energy and semi-major axes of each planet are conserved to the lowest order. The orbit-averaged Hamiltonian (H) can be calculated semi-analytically using the disturbing functions of planets (e.g., Brouwer & Clemence 1961) and equation (D1). Expanding to the second order of the eccentricities, we find

$$H = \frac{M_c n_c^2 a_c^2}{2} + \frac{M_d n_d^2 a_d^2}{2} + \frac{n_c a_c^2 N_c}{2t_c} + \frac{n_d a_d^2 N_d}{2t_c} + \frac{GM_c M_d a_c}{8a_d^2} \left\{ b_{3/2}^{(1)}(e_c^2 + e_d^2) - 2b_{3/2}^{(2)} e_c e_d \cos \eta \right\}. \quad (\text{D3})$$

From the conservation of the total angular momentum, a relation

$$J \equiv M_c n_c a_c^2 \sqrt{1 - e_c^2} + M_d n_d a_d^2 \sqrt{1 - e_d^2} = \text{constant} \quad (\text{D4})$$

holds provided their orbital planes are not inclined from each other. Thus, to second order in eccentricity,

$$\frac{n_c a_c^2 N_c}{t_c} + \frac{n_d a_d^2 N_d}{t_c} + \frac{GM_c M_d a_c}{4a_d^2} \left\{ b_{3/2}^{(1)}(e_c^2 + e_d^2) - 2b_{3/2}^{(2)} e_c e_d \cos \eta \right\} = \text{constant}, \quad (\text{D5})$$

$$M_c n_c a_c^2 e_c^2 + M_d n_d a_d^2 e_d^2 = \text{constant}, \quad (\text{D6})$$

for any given values of H and J . Divided equation (D5) with equation (D6), we find that

$$\frac{x^2(1 + N_c) + 2Cx \cos \eta + (\gamma_d^{-1} + N_d)}{\gamma_d x^2 + 1} = \text{constant}, \quad (\text{D7})$$

and obtain the equi-Hamiltonian contour lines for various values of the constants of integration. In equation (D7), the masses of the disk and planets are contained only in the form of their ratios. Therefore, as long as $M_* \gg M_{c,d}$, the equi-Hamiltonian contours are not affected by the obliquity i of the system. We show below that other than small deviations due to non-linear effects, the planets' orbits closely follow the contours in the equi-Hamiltonian map.

REFERENCES

- Artymowicz, P. 1993, *PASP*, 105, 1032
- Barnes, R., & Quinn, T. 2001, *ApJ*, 550, 884
- Beckwith, S. 1999, in *Origin of Stars and Planetary Systems*, ed. C. J. Lada & N. Kylafis, (Dordrecht: Kluwer), 579
- Binney, J., & Tremaine, S. 1987, *Galactic Dynamics* (Cambridge: Cambridge Univ. Press)
- Bodenheimer, P., & Pollack, J. B. 1986, *Icarus*, 67, 391
- Brouwer, D., & Clemence, G. M. 1961, in *Methods of Celestial Mechanics* (New York: Academic Press)
- Bryden, G., Chen, X., Lin, D. N. C., Nelson, R. P., & Papaloizou, J. C. B. 1999, *ApJ*, 514, 344
- Bryden, G., Rzyczka, M., Lin, D. N. C., & Bodenheimer, P. 2000, *ApJ*, 540, 1091
- Butler, R. P., Marcy, G. W., Fischer, D. A., Brown, T. M., Contos, A. R., Korzennik, S. G., Nisenson, P., & Noyes, R. W. 1999, *ApJ*, 526, 916
- Chambers, J. E., Wetherill, G. W., & Boss, A. P. 1996, *Icarus*, 119, 261
- Chiang, E. I., & Murray, N. 2002, *ApJ*, 576, 473
- Chiang, E. I., Tabachnik, S., & Tremaine, S. 2002, *ApJL*, submitted
- Goldreich, P., & Sari, R. 2002, *ApJ*, submitted
- Goldreich, P., & Tremaine, S. 1979, *Nature*, 277, 97
- Goldreich, P., & Tremaine, S. 1980, *ApJ*, 241, 425
- Goldstein, H. 1980, in *Classical Mechanics* (Reading: Addison Wesley)
- Haisch, K. E. Jr., Lada, E. A., & Lada, C. J. 2001, *ApJ*, 553, 153
- Hayashi, C. 1981, *Prog. Theor. Phys. Suppl.*, 70, 35
- Hayashi, C., Nakazawa, K., & Nakagawa, Y. 1985, in *Protostars and Planets II*, ed. by D. C. Black and M. S. Matthews (Tucson: Univ. of Arizona Press), 1100
- Heppenheimer, T. A. 1980, *Icarus*, 41, 76
- Ito, T., & Miyama, S. M. 2001, *AJ*, 551, 372
- Kinoshita, H., & Nakai, H. 2000, in *ASP Conf. Ser.*, s202, *Planetary Systems in the Universe*, ed. A. J. Penny, P. Artymowicz, A. -M. Lagrange, and S. S. Russell (San Francisco: ASP), in press
- Laughlin, G. & Adams, F. C., 1999, *ApJ*, 526, 881

- Lin, D. N. C., & Ida, S. 1997, *ApJ*, 477, 781
- Lin, D. N. C., & Papaloizou, J. C. B. 1980, *MNRAS*, 191, 37
- Lin, D. N. C., & Papaloizou, J. C. B. 1986a, *ApJ*, 307, 395
- Lin, D. N. C., & Papaloizou, J. C. B. 1986b, *ApJ*, 309, 846
- Lin, D. N. C., & Papaloizou, J. C. B. 1993, in *Protostars and Planets III*, ed. E. H. Levy and J. I. Lunine (Tucson: Univ. of Arizona Press), 749
- Lissauer, J. J. 1987, *Icarus*, 69, 249
- Lissauer, J. J., & Rivera, E. J. 2001, *ApJ*, 554, 1141
- Marcy, G. W., & Butler, R. P. 2000, *PASP*, 112, 137
- Marcy, G. W., Butler, R. P., Vogt, S. S., Liu, M. C., Laughlin, G. Apps, K., Graham, J. R., Lloyd, J., Luhman, K. L., & Jayawardhana, R. 2001, *ApJ*, 555, 418
- Mardling, R., & Lin, D. N. C. 2002, *ApJ*, 573, 829
- Mardling, R., & Lin, D. N. C. 2003, *ApJ*, submitted
- Mizuno, H. 1980, *Prog. Theor. Phys. Suppl.*, 64, 544
- Murray, C. D., & Dermott, S. F. 1999, in *Solar System Dynamics* (Cambridge: Cambridge Univ. Press)
- Nagasawa, M., Tanaka, H., & Ida, S. 2000, *AJ*, 119, 1480
- Nagasawa, M., & Ida, S. 2000, *AJ*, 120, 3311
- Papaloizou, J. C. B., & Lin, D. N. C. 1984, *ApJ* 285, 818
- Papaloizou, J. C. B., Nelson, R. P., & Masset, F. 2001, *A&A* 366, 263
- Pollack, J. B., Hubickyj, O., Bodenheimer, P., Lissauer, J. J., Podolak, M., & Greenzweig, Y. 1996, *Icarus*, 124, 62
- Rasio, F. A., Tout, C. A., Lubow, S. H., & Livio, M. 1996, *ApJ*, 470, 1187
- Rivera, E. J., & Lissauer, J. J. 2000, *ApJ*, 530, 454
- Savonije, G. J., Papaloizou, J. C. B., & Lin, D. N. C. 1994, *MNRAS*, 268, 13
- Stepinski, T. F., & Black, D. C. 2001, *A&A*, 371, 250
- Stepinski, T. F., Malhotra, R., & Black, D. C. 2000, *ApJ*, 545, 1044
- Takeuchi, T., Miyama, S. M., & Lin, D. N. C. 1996, *AJ*, 460, 832
- Ward, W. R., Colombo, G., & Franklin, F. A. 1976, *Icarus*, 28, 441
- Ward, W. R. 1981, *Icarus*, 47, 234

Weidenschilling, S. J., & Marzari, F. 1996, *Nature*, 384, 619

Wetherill, G. W. 1990, *AREPS*, 18, 205

Williams, J. G. 1969, Ph. D. thesis, Univ. of California, Los Angeles

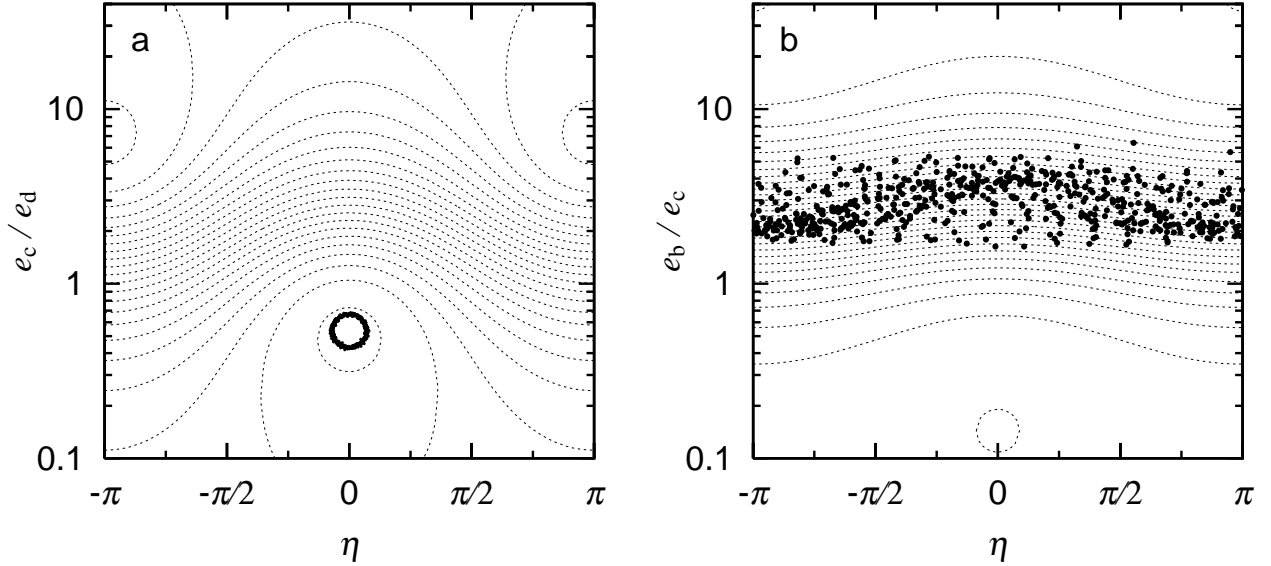


Fig. 1.— Orbital evolutions of extra solar planets. Points show the orbits obtained from numerical simulations. The dotted lines are the equi-Hamiltonian contours of the planetary system. The contours are spaced with equal intervals. (a)Orbital evolution of planets c and d (points) of Upsilon Andromedae system. Orbits are integrated for 2×10^4 years starting from present orbital elements. The period of the libration is about 6000 years. (b)Orbital evolution of planets b and c (points) of HD168443 system. Orbits are integrated for 2.5×10^4 years. The circulation period for η to evolve from $-\pi$ to π is about 16000 years.

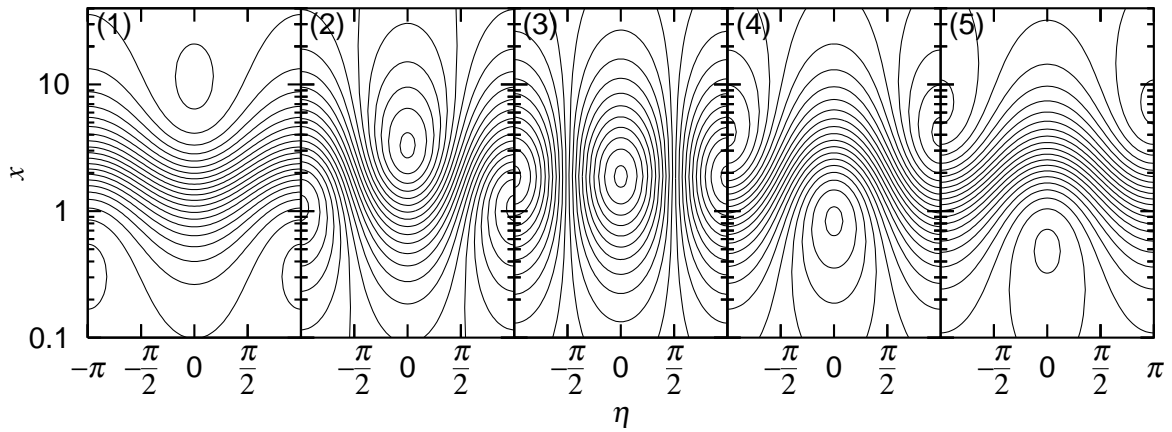


Fig. 2.— Equi-Hamiltonian contours of Upsilon Andromeda planetary system in $(x-\eta)$ diagram. The time sequence of nebula depletion proceeds from panel (1) to (5). The nebula edge is set to be (1) 4.2AU, (2) 5AU, (3) 5.5AU, (4) 7AU, and (5) infinity (the present disk-free planetary system).

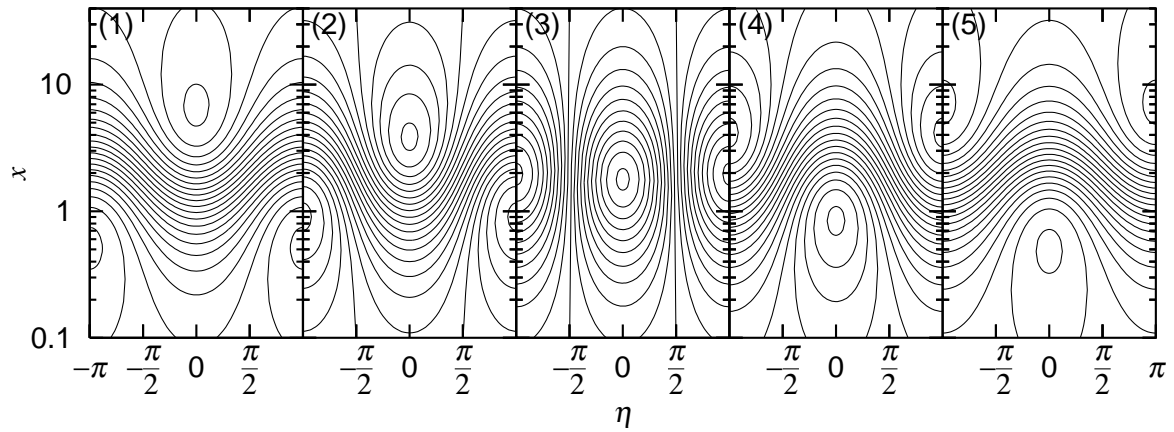


Fig. 3.— Equi-Hamiltonian contours of Upsilon Andromeda planetary system in $(x-\eta)$ diagram. The time sequence of nebula depletion proceeds from panel (1) to (5). The depletion ratio $\exp(-t/t_{\Delta N})$ is at (1)1, (2) 0.75, (3) 0.5, (4) 0.25, and (5) 0. The disk edge is located at 4.5AU.

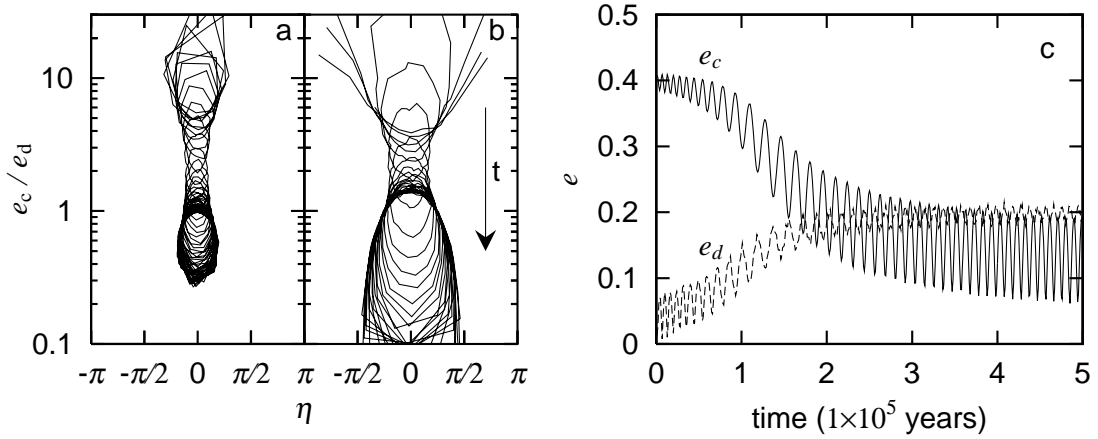


Fig. 4.— Orbital evolutions of planets during the depletion of the protoplanetary disk. (a) In this system, planets were initially on a librating track in the $(x-\eta)$ diagram and remained on a librating track with a high e_d after their nascent disk is completely depleted. The initial magnitude of $x = 8$ and $\eta = \pi/4$ prior to the epoch of the disk depletion. (b) In this system, planets were initially on a circulating track in the $(x-\eta)$ diagram but entered on a librating track after the disk is completely depleted. The initial magnitude of $e_c = 0.4$, $e_d = 0.05$, and $\eta = 3\pi/2$ prior to the disk depletion. (c) The evolution of the eccentricities in the case of (a). The solid and dashed lines show the eccentricity of planet c and d, respectively. The retreating speed of nebula edge is $10^{-5}(\text{AU year}^{-1})$, and the nebula edge is 4.2 AU at $t = 0$.

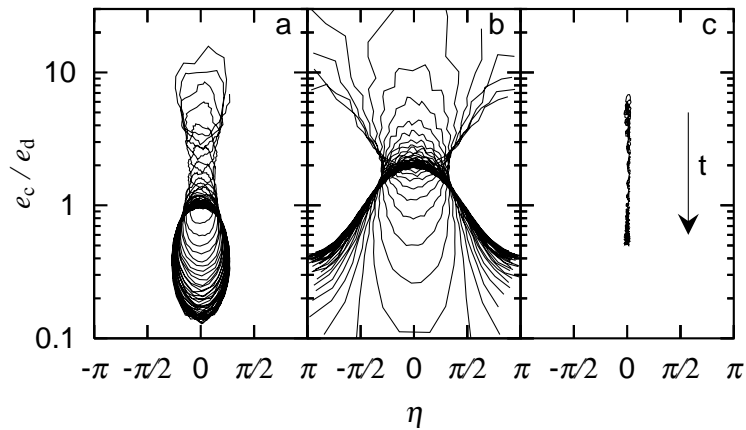


Fig. 5.— The orbital evolutions of planets during the uniform depletion of the protoplanetary disk. (a) In this system, planets were initially on a librating orbit. The initial condition is the same as the case of Figure 4a. (b) In this system, planets were initially on an open circulating track and remained on an open circulating track after the disk is completely depleted. The initial magnitude of $e_c = 0.4$, $e_d = 0.05$, and $\eta = \pi$. (c) In this system, the coincidence of the periastrons is preserved. The magnitude of $e_c = 0.45$, $e_d = 0.08$, and $\eta = 0$ initially. In these calculations, the nebula edge is set to be 4.5 AU, and $t_{\Delta N} = 10^5$ years.

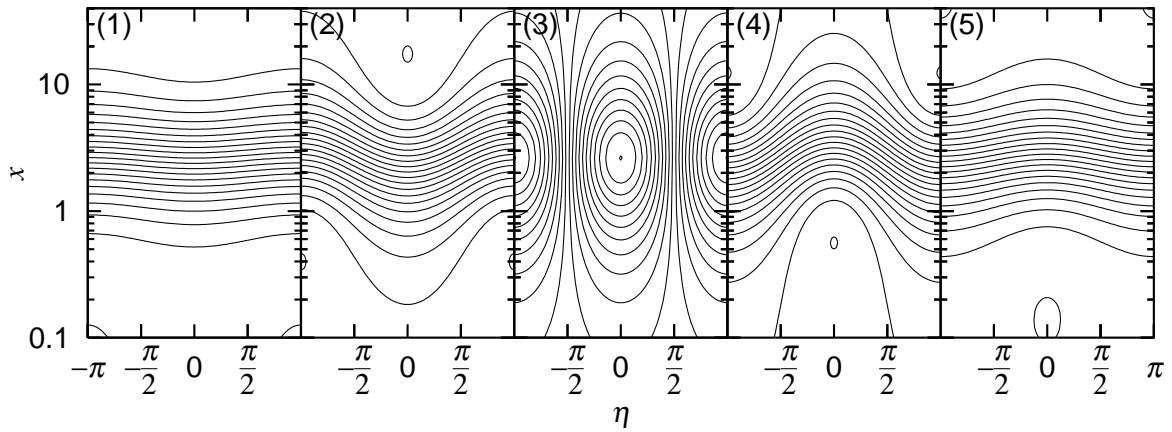


Fig. 6.— Equi-Hamiltonian contours of HD168443 planetary system in the $(x-\eta)$ diagram. The time sequence of the nebula depletion proceeds from panel (1) to (5). The nebula edge is at (1) 5AU, (2) 6.5AU, (3) 7.2AU (secular resonance) (4) 8AU, and (5) infinity (present planetary system).

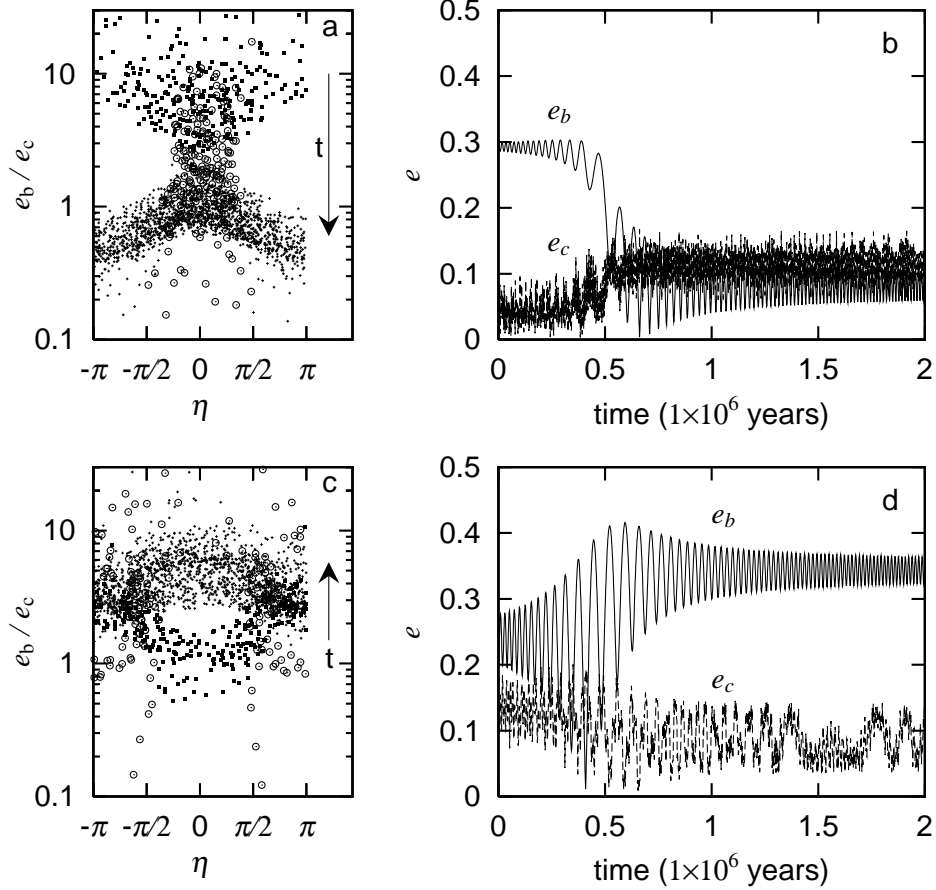


Fig. 7.— Orbital evolutions of HD168443 planets during the uniform depletion of the protoplanetary disk. The edge of the disk is located at $r_{\text{edge}} = 5.5\text{AU}$. The disk depletion timescale is $t_{\Delta N} = 10^6$ years. (a) The orbital evolution in the $(x-\eta)$ diagram for the case with the initial values of $x = 6$ and $\eta = 0$. The eccentricity ratio for the first $t = 4 \times 10^5$ years is denoted by filled squares and that for $t = 4 \times 10^5 \sim 7 \times 10^5$ years (around the secular resonance) is denoted by open circles and that for $t > 7 \times 10^5$ years are shown by small plus symbols. (b) The evolution of eccentricities corresponds to the system of planets in panel a. (c) The evolution of the eccentricity ratio for the case with the initial values of $x = 1$ and $\eta = 0$. Filled squares, open circles, and small plus show the period of time before 4×10^5 , during $4 \times 10^5 \sim 6.2 \times 10^5$, and after 6.2×10^5 years, respectively.

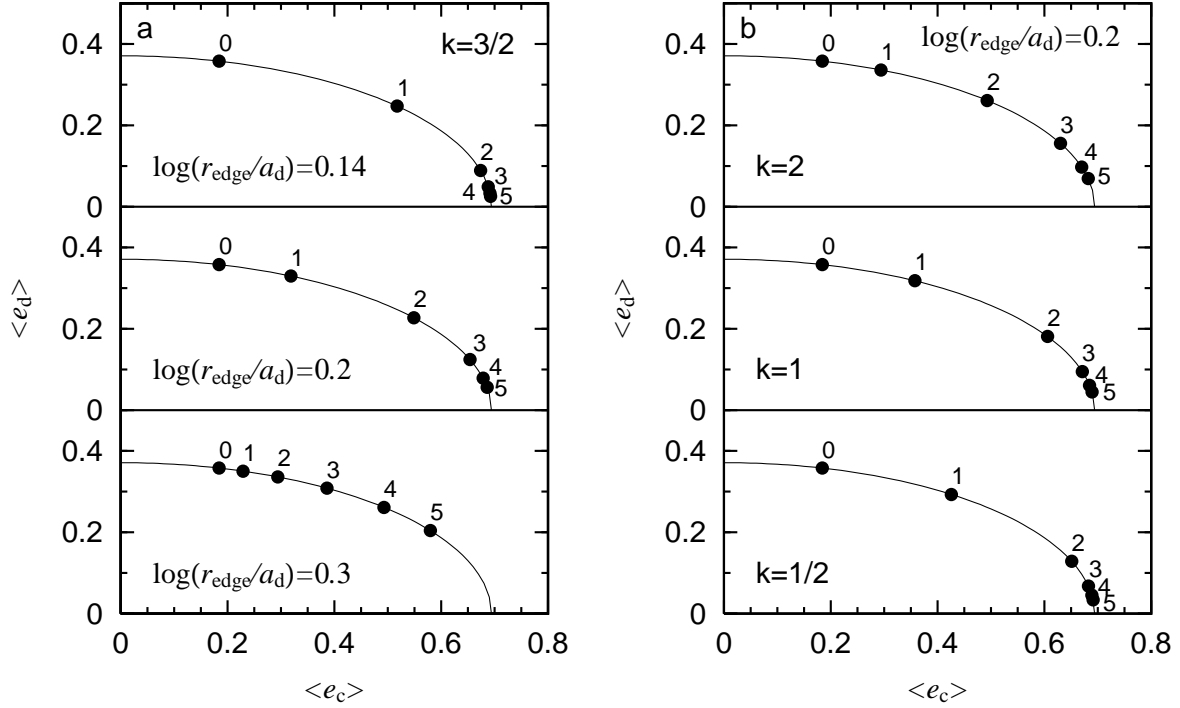


Fig. 8.— Initial eccentricities of planets c and d around Ups And. The eccentricities e_c and e_d are shown by filled circle for five different initial disk mass. The number along the filled circle shows the surface density (e.g., '5' means $5 \sin i \times$ of the minimum mass model). (a) The locations of the disk edge are $\log(r_{\text{edge}}/a_d) = 0.14$ (top panel), 0.2 (middle panel), 0.3 (bottom panel). (b) The surface density gradients are $k = 3/2$ (top panel), $k = 1$ (middle panel), $k = 1/2$ (bottom panel). The location of the disk edge is 4.057AU.

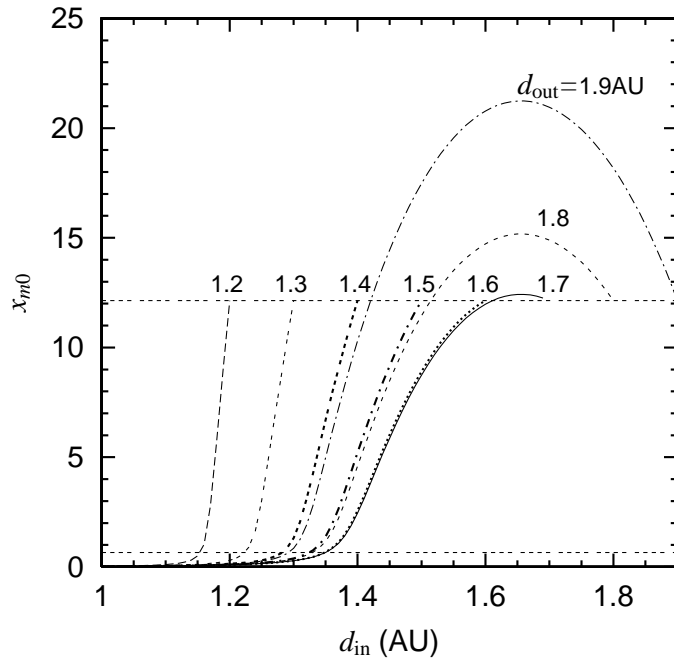


Fig. 9.— The location of the librating center around zero (x_{m0}) in the case that there is a ring between the planets c and d around Ups And. The ring’s surface density is set to be $5 \sin i$ times that of the minimum mass model and it is confined between d_{in} and d_{out} . Eight lines for different values of d_{out} are shown. The horizontal line at ~ 12 shows the x_{m0} without the disk. The horizontal line at 0.66 shows the current x_{m0} .

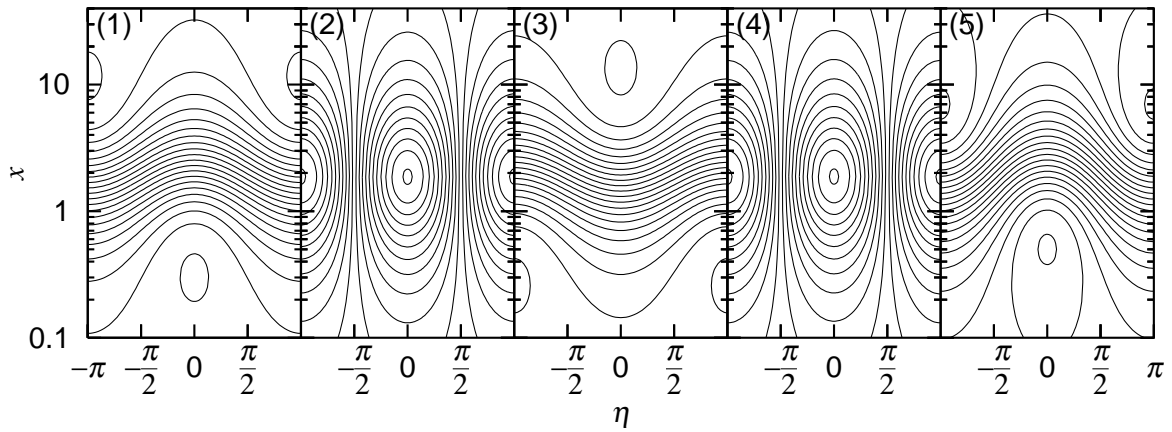


Fig. 10.— Equi-Hamiltonian contours of Ups And planetary system. The surface densities of residual ring and the disk are (1)100% , (2) 53% (ring) and 100% (disk), (3) 0% (ring) and 100% (disk), (4) 0% (ring) and 35% (disk), and (5)0% of their initial values, respectively.

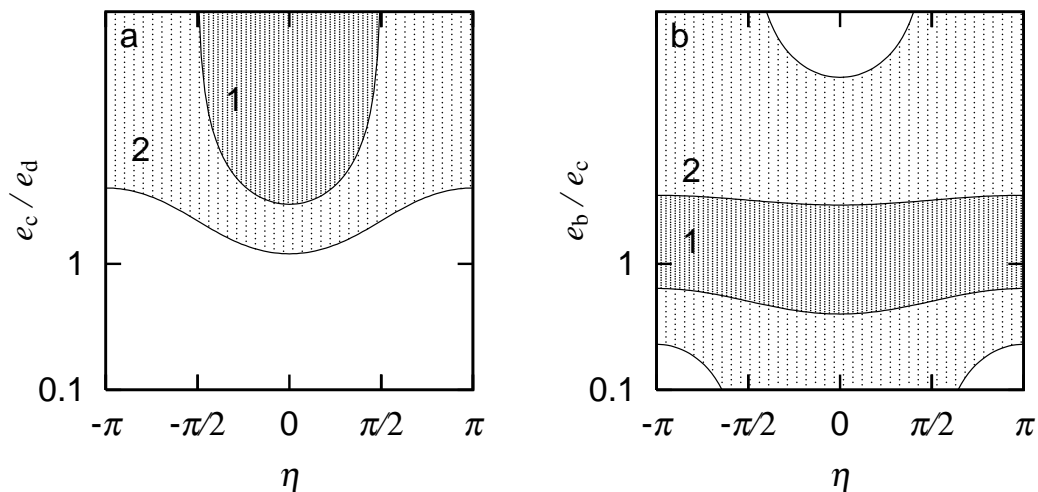


Fig. 11.— (a) A schematic diagram of the $(x-\eta)$ plane for the system of planets around Ups And. Planets which initially occupy region 1, enter into a librating track in the $(x-\eta)$ plane after the disk depletion. Their orbits become similar to present orbits of planets c and d. For planets which initially occupy region 2, their eccentricity ratio is reduced after the disk depletion. (b) A schematic diagram of the $(x-\eta)$ plane for the planetary systems around HD168443. Planets which initially occupy region 2, enter into the open circulating tracks in the $(x-\eta)$ plane after the disk depletion. Planets which initially occupy region 1 evolve into orbits similar to those observed around HD168443.

Table 1. Orbital parameters of extrasolar multiple planets planets

planets	$a(\text{AU})$	e	$\varpi(\text{rad})$	$M \sin i(M_J)$	T_{peri}
(a) Upsilon Andromedae ($M_* = 1.3M_\odot$)					
planet b	0.059	0.01	5.522	0.69	2450000.6383
planet c	0.827	0.23	4.314	2.06	2450399.0
planet d	2.56	0.35	4.374	4.10	2451348.9
(b) HD168443 ($M_* = 1.01M_\odot$)					
planet b	0.295	0.53	3.018	7.73	2450047.58
planet c	2.87	0.20	1.098	17.15	2450250.6
(c) HD74156 ($M_* = 1.05M_\odot$)					
planet b	0.276	0.649	3.206	1.56	2451981.4
planet c	3.47	0.395	4.189	>7.5	2450849
(d) 47 UMa ($M_* = 1.03M_\odot$)					
planet b	2.09	0.061 ± 0.014	3.00 ± 0.26	2.54	2453622 ± 34
planet c	3.73	0.1 ± 0.1	2.22 ± 0.98	0.76	2451363.15 ± 493
(e) HD12661 ($M_* = 1.07M_\odot$)					
planet b	0.804	0.35	5.11	2.21	2460208.393
planet c	2.652	0.11	2.29	1.58	2459398.08

References. — <http://exoplanets.org/almamacframe.html>

Table 2. Notations

Symbol	meaning
C	$-5a_c/(4a_d)$
γ_d	$(a_c/a_d)^{1/2}(M_c/M_d)$
ϵ	$x/x_m - 1$
η	$\varpi_c - \varpi_d$
t_c	$(4/3n_c)(M_*/M_d)(a_d/a_c)^3$
x	e_c/e_d
x_m	values of x at centers of librating orbits
ΔN	$d\eta/d\tau$ caused by the disk potential (eq. [A3])